Power Loss Reduction and Voltage Profile Improvement Using Optimal Placement of Distributed Generation and DSTATCOM in Radial Distribution System (Case study: Adama Substation II)

Feyisa Hailu Esho

A Thesis Submitted to the Department of Electrical Power and Control Engineering

School of Electrical Engineering and Computing

Presented in Partial Fulfillment of the Requirement for the Degree of Master's in Power Systems Engineering

Office of Graduate Studies

Adama Science and Technology University

June, 2024

Adama, Ethiopia

Power Loss Reduction and Voltage Profile Improvement Using Optimal Placement of Distributed Generation and DSTATCOM in Radial Distribution System (Case study: Adama Substation II)

Feyisa Hailu Esho

Advisor: Dr. Tefera Terefe

Co-advisor: Mesfin Megra (MSc.)

A Thesis Submitted to the Department of Electrical Power and Control Engineering

School of Electrical Engineering and Computing

Presented in Partial Fulfillment of the Requirement for the Degree of Master's in Power Systems Engineering

Office of Graduate Studies

Adama Science and Technology University

June, 2024

Adama, Ethiopia

DECLARATION

I hereby declare that this Master Thesis entitled "**Power Loss Reduction and Voltage Profile Improvement Using Optimal Placement of Distributed Generation and DSTATCOM in Radial Distribution System (Case study: Adama Substation II)**" is my original work. That is, it has not been submitted for the award of any academic degree, diploma or certificate in any other university. All sources of materials that are used for this thesis have been duly acknowledged through citation.

Feyisa Hailu Esho	__________________	________________
Name of student	Signature	Date

RECOMMENDATION

We, the advisor(s) of this thesis, hereby certify that we have read the revised version of the thesis entitled "**Power Loss Reduction and Voltage Profile Improvement Using Optimal Placement of Distributed Generation and DSTATCOM in Radial Distribution System (Case study: Adama Substation II)**" prepared under our guidance by **Feyisa Hailu Esho** submitted in partial fulfillment of the requirements for the degree of Master's of Science in Power Systems Engineering. Therefore, I/we recommend the submission of revised version of the thesis to the department following the applicable procedures.

Dr. Tefera Terefe	____________________	_____________
Major Advisor	Signature	Date
Mesfin Megra (MSc.)	___________________	_____________
Co-advisor	Signature	Date

APPROVAL PAGE

We, the advisors of the thesis entitled "**Power Loss Reduction and Voltage Profile Improvement Using Optimal Placement of Distributed Generation and DSTATCOM in Radial Distribution System (Case study: Adama Substation II)**" and developed by **Feyisa Hailu Esho**, hereby certify that the recommendation and suggestions made by the board of examiners are appropriately incorporated into the final version of the thesis.

Dr. Tefera Terefe	________________	______________
Major Advisor	Signature	Date
Mesfin Megra (MSc.)	________________	______________
Co-advisor	Signature	Date

We, the undersigned, members of the Board of Examiners of the thesis by Feyisa Hailu Esho have read and evaluated the thesis entitled "**Power Loss Reduction and Voltage Profile Improvement Using Optimal Placement of Distributed Generation and DSTATCOM in Radial Distribution System (Case Study: Adama Substation II)**" and examined the candidate during open defense. This is, therefore, to certify that the thesis is accepted for partial fulfillment of the requirement of the degree of Master of Science in Power Systems Engineering.

____________________	________________	______________
Chairperson	Signature	Date
____________________	________________	______________
Internal Examiner	Signature	Date
Dr.Yeshitela Shiferaw		06/20/2024
External Examiner	Signature	Date

Final approval and acceptance of the thesis is contingent upon submission of its final copy to the Office of Postgraduate Studies (OPGS) through the Department Graduate Council (DGC) and School Graduate Committee (SGC).

____________________	________________	______________
Department Head	Signature	Date
____________________	________________	______________
School Dean	Signature	Date
____________________	________________	______________
Office of Postgraduate Studies, Dean	Signature	Date

ACKNOWLEDGEMENT

First and foremost, I would like to express my deepest gratitude to God Almighty for His guidance and blessings throughout my academic journey.

I am deeply grateful to my esteemed advisor, Dr. Tefera Terefe, for his invaluable mentorship, support, and encouragement. Your expertise and dedication have been instrumental in the completion of this thesis. I am also grateful to my co-advisor, Mr. Mesfin Megra, for his guidance and insights. Your contributions have greatly enriched my research experience.

I would like to thank the staff members of the Adama substation I and II, and the Ethiopian Electric Utility (EEU) Adama district for their invaluable support in providing me with essential data and their warm hospitality. I am also indebted to Adama Science and Technology University for providing the financial support that made this research possible.

Finally, I would like to express my deepest gratitude to my beloved mother and father, and to my cherished sister and brother, whose unwavering love and sacrifices have been the cornerstone of my success. I am also deeply grateful to my dear friends, whose companionship and support have made this journey all the more meaningful.

TABLE OF CONTENTS

LIST OF TABLES

LIST OF FIGURES

LIST OF ACRONYMS AND ABBREVIATIONS

AI	Artificial Intelligence
ASTU	Adama Science and Technology University
BCBV	Branch Current Bus Voltage
BFOA	Bacterial Foraging Optimization Algorithm
BFS	Backward/Forward Sweep
BIBC	Branch Injection Branch Current
DG	Distributed Generation
DLF	Direct Load Flow
DSTATCOM	Distribution Static Compensator
EEU	Ethiopian Electric Utility
EEP	Ethiopian Electrical Power
FACTS	Flexible Alternating Current Transmission System
GA	Genetic Algorithm
GMR	Geometric Mean Radius
KCL	Kirchhoff’s Current Law
LSF	Loss Sensitivity Factor
PSI	Power Stability Index
PV	Photovoltaic
RDS	Radial Distribution System
SSSC	Static Synchronous Series Compensator
SVC	Static Var Compensator
STATCOM	Static Synchronous Compensator
TAPL	Total Active Power Loss
TRPL	Total Reactive Power Loss

TCPST	Thyristor-Controlled Phase Shifting Transformer
TCSC	Thyristor Controlled Series Compensator
TRPL	Total Reactive Power Loss
UPFC	Unified Power Flow Controller
VSI	Voltage Stability Index

ABSTRACT

The electric power system network comprises distribution, transmission, and generation components. The distribution system connects high-voltage transmission networks with the end users. Power plants are often located far from consumers. This leads to a significant power loss in both transmission and distribution systems. Since, the distribution system has a low X/R ratio and operates at low voltage, losses in the distribution system are typically greater than losses in the transmission system. The main objective of this work is voltage profile enhancement and minimization of power losses by integrating Distributed Generation (DG) and Distribution Static Synchronous Compensator (DSTATCOM) to Adama substation II feeder L2. Adama substation II feeder L2 is selected due to its high power demand, high permanent overload power interruption, *and cover large areas. DG and DSTATCOM devices have been designed and integrated into the Adama substation II feeder L2. This integration has resulted in an enhanced voltage profile and reduced power loss in the distribution system. In this work, the Direct Load Flow (DLF) technique was employed to calculate the load flow. Particle Swarm Optimization (PSO) algorithm was employed to determine the optimal place and size of DG and DSTATCOM devices. The proposed systems were analyzed and simulated using the MATLAB simulation tool. The performance of the distribution system was evaluated under different cases: base case, with DG only, and with both DG and DSTATCOM. The Integration of three DG and one DSTATCOM into the system enhances the minimum voltage profile from* 0.75141 to 0.9544 and reduces the active and reactive power losses by 84.67% and 83.09%, respectively. *Finally, the study analyzes the economic viability of DG and DSTATCOM integration, considering investment costs and payback period. The findings suggest that installing these devices is a cost-effective solution for enhancing the voltage profile and reducing the power loss of the distribution system.*

Keywords: *DG, DSTATCOM, MATLAB, Optimum location, Optimum size, PSO, Power loss, Voltage Profile.*

CHAPTER ONE

1. INTRODUCTION

1.1. Background of the Study

The electric power system network comprises distribution, transmission, and generation components. In these well-known components, the distribution system is the most crucial and the weakest one in the electric power system. The distribution system can be a radial, ring, or interconnected structure. The distribution system is usually designed in a radial structure because of its simplicity and low cost compared to other structures. It consists of commercial, industrial, and residential loads, as well as it has a low X/R ratio compared to transmission systems. So, the radial distribution system (RDS) has high power loss, high interruption, poor voltage profile, and voltage stability (Alyu et al., 2023).

When compared to others, distribution systems experience a high loss of power due to their operation at low voltage. Voltage drop is also a common issue in distribution systems. Distribution feeders may supply or absorb reactive power depending on the load current. When the load on a feeder is less than the surge impedance, the feeder acts as a source of reactive power, supplying it to the system. However, when the load exceeds the surge impedance, the feeder absorbs reactive power from the system. Consequently, voltage drop issues may emerge when feeding heavy loads or employing long-distance distribution feeders (Taye, 2019).

The power distribution system experiences significant power losses (approximately 13% of the total generated power), primarily within distribution networks (Salkuti, 2021). Additionally, radial distribution systems (RDSs) are prone to voltage profile problems, requiring immediate attention. To minimize the active and reactive line losses and increase the efficiency of the distribution system, it is essential to maintain the voltage at equipment terminals within permissible limits, so the reactive power flow is limited (Sirjani & Rezaee Jordehi, 2017).

A distribution system is one of the most crucial components of a power system utilized to transport electrical energy to end users is the electric power distribution system. Thus, utilities have the essential responsibility of delivering reliable, efficient, and economical services to their customers. They must ensure that the voltage and power quality supplied meet the necessary standards and provide continuous and satisfactory service.

Distribution generation (DG) refers to small-scale renewable energy resources such as wind, solar photovoltaic (PV), biomass, etc. that are optimally placed to meet the required demand and thereby reduce losses in the distribution system. However, the deployment of DG alone is insufficient to meet reactive power demands, causing under voltage at multiple buses. To mitigate this issue, DSTATCOMs are strategically placed to optimize voltage levels (Iqbal et al., 2018). Integrating DG and DSTATCOM units into the distribution system is not a simple decision; thus, the positioning and sizing of these units must be carefully considered to enhance the voltage profile and decrease the power loss. Researchers have developed various optimization techniques to find the optimal place and size of DG and DSTATCOM units in electrical distribution networks to minimize power loss and enhance the voltage profile.

Particle swarm optimization (PSO) is an artificial intelligence (AI) algorithm that was developed by Kennedy and Eberhart in 1995(Tungadio et al., 2015). A power system is one of the possible areas in which PSO can be employed to meet the highest standards. This paper demonstrates power loss reduction and voltage profile improvement and, PSO is utilized to find the optimal place and size of DG and DSTATCOM.

1.2. Statement of the Problem

Electrical power demand is steadily rising from time to time, and distribution feeders that transmit power from substations to customers are becoming overloaded beyond their intended capacity. Long-distance distribution feeders that are overloaded experience significant power losses and voltage profile degradation. Therefore, it's crucial to find ways to reduce power losses and improve voltage profiles in the distribution network. Various techniques such as conductor grading, network reconfiguration, Distributed Generation (DG) placement, and FACTS devices placement, can be employed to reduce the power loss and fluctuation of voltage in a distribution feeder. From those techniques integrating DG and DSTATCOM is commonly used in Distribution system. Adama substation II feeder L2 covers large areas and experiences high power demand, and due to overload, interruption occurs frequently with a significant voltage drop.

This thesis focuses on the power loss minimization and enhancement of the voltage profile of the Adama substation II feeder L2 distribution system by optimally placing DG and DSTATCOM using a PSO method. The PSO optimization technique is employed to find the optimal size and place of DG and DSTATCOM.

1.3. Objectives

1.3.1. General Objectives

The main objective of this thesis work is to enhance power loss reduction and improve voltage profile in a radial distribution system through the optimal placement of DG and DSTATCOM.

1.3.2. Specific Objectives

The specific objectives of this proposal are:

- To assess the existing power loss and voltage profile in the radial distribution system at Adama substation II feeder L2.
- To obtain mathematical modeling of DG and DSTATCOM for Adama substation II feeder L2.
- To find the optimal size and place of DG and DSTATCOM using the PSO methods.
- To evaluate system performance at base case, with DG only, and with DG and DSTATCOM.
- To estimate the investment cost of DG and DSTATCOM.

1.4. Significant of the Study

This study significantly contributes to finding the best way to lower distribution losses and improve the voltage profile. The output of this study is believed to be very significant to both customers and the Ethiopian Electric Utility (EEU).

In addition to this, the study output will have the following contributions.

- Minimize distribution losses and improve voltage profile by allocating DG and DSTATCOM into Adama Substation II feeder L2.
- The study utilized direct load flow which is fast.
- The PSO optimization technique is suggested to determine the optimal size and place of DG and DSTATCOM.

1.5. Scope of the Study

This work has focused on studying and analyzing power loss minimization and improvement of voltage profile in Adama substation II feeder L2 by integrating DG and DSTATCOM. Additionally, the study investigates the current substation voltage profile, and power loss, and the percentage of improvements that can be gained by integrating DG and DSTATCOM into the present Adama substation II feeder L2. Also, the investment cost analysis of DG and DSATCOM installation was studied. The study utilized M

ATLAB simulation tools to simulate the suggested system.

1.6. Limitation of the Study

This thesis work has been limited to the mathematical modeling and simulation of the suggested system using MATLAB simulation tools, for voltage profile enhancement and power loss minimization by integrating DG and DSTATCOM into the system. The study considers the impact of DG and DSTATCOM on power loss and voltage profile only. Additionaly, while PSO is powerful optimization technique, it might not be the absolute best solution, and limitations in the search space could restrict finding of the optimal DG and DSTATCOM placement and sizing.

1.7. Thesis Outline

This thesis is organized into five chapters

A brief background, statement of the problem, objectives of the study, significance of the study, scope of the study, and research limitation are covered in Chapter 1 of the research. Chapter 2 presents the theoretical background and discusses previous literature relevant to the topics of voltage profile enhancement and power loss reduction of distribution networks. Chapter 3 provides a detailed explanation of the methodology and approaches, starting with a site description data collection, and data analysis. In Chapter 4, the presentation and discussions of the simulation result are conducted. Finally, in Chapter 5, the research's conclusion and recommendations were addressed.

CHAPTER TWO

2. THEORETICAL BACKGROUND AND LITERATURE REVIEW

2.1. Introduction

Electrical power is the largest and most complex system, which is a vital element of any modern economy. Electricity can be transported from generating stations to customers through a network of interconnected power lines called an electrical grid. The electrical grid is made up of generating stations that generate electricity, as well as transmission lines that deliver electricity from the generating station to distribution substations, and distribution lines that transport electricity from the distribution substation to end users. Within the substation, high-voltage power is stepped down to medium and low-voltage power using step-down transformers and delivered to customers through various distribution feeders (Mihret Desta, 2019).

2.2. Electric Power Distribution System

The distribution system is the final step of the electricity supply chain; it transports electricity from the distribution substation to the customers. Medium-voltage electricity is carried to nearby distribution transformers through primary distribution lines. These lines connect the distribution substation to the distribution transformers, forming the primary distribution network. From the distribution transformers, low-voltage electricity flows to end-consumers through secondary or distribution feeders. Power is supplied to both the primary and secondary distribution lines at standard voltage levels.

The 45 kV, 33 kV, or 15 kV electrical power distribution network in Ethiopia is categorized as medium voltage. Typically, 33kV and 15kV overhead cables are used to provide power to as many as 80 step-down distribution transformers on each of the 33kV and 15kV circuits. Before reaching the consumer, the voltage is stepped down to 380 volts for three-phase systems or 220 volts for single-phase systems (Mihret Desta, 2019).

All distribution system connections of electric power are done by a constant voltage level throughout the system. Common distribution circuit configurations include: Radial distribution system, Ring distribution system, and interconnected distribution system.

2.2.1. Radial Distribution System

In this system, multiple distribution feeders originate from a single substation and feed electricity to distributors, with each distributor receiving power from only one end of the distribution feeders. This system is widely used because of its simple design and affordable construction costs (Alyu et al., 2023). A radial system, being connected only to one source of supply, is susceptible to voltage fluctuations and various interruptions. Unlike feeders with alternative supply capabilities, radial feeders generally experience voltage fluctuations and lower reliability.

2.2.2. Ring Distribution System

The primary feeders of the distribution substation in this system are arranged in a loop configuration. The loop circuit starts from the bus bars at the substation, extends through the designated area, and then returns to the substation. One of the key benefits of the ring main system is that it minimizes the impact of voltage fluctuations on consumer terminals.

2.2.3. Interconnected Distribution System

An interconnected distribution system refers to the energizing of the ring feeder by multiple generating stations or substations. In this system, if one substation is unable to handle the high demand, the other substation can step in and ensure that there is no interruption in the power supply. This redundancy helps to maintain a reliable and consistent flow of electricity to the customers.

2.3. Power Loss and Voltage Profile

Power loss is the wastage of electrical energy and is caused by the conductor impedance. It is directly proportional to the square of the current flowing through it. Various factors such as load level, length of distribution lines, transformers, size of conductors, etc., influence power losses in distribution systems. Electrical systems experience two types of power losses: atual power loss and reactive power loss. Line resistance causes actual power loss, on the other hand, reactive components cause reactive power loss. Utility companies generally prioritize actual power loss because it directly impacts the efficiency of delivering energy to customers. On the other hand, reactive power loss is also significant.

The voltage profile in a power distribution system refers to the variation of voltage magnitude along the distribution line. It is crucial because electrical equipment needs to operate near their rated voltage for optimal performance. Factors such as load demand, line impedance, etc., can influence the voltage profile. If the voltage deviates significantly from the rated value, it can lead to inefficient operation or even damage to the equipment. Therefore, maintaining an appropriate voltage profile is crucial to power system management.

2.4. Techniques for Improving Voltage Profile and Reducing Power Loss

As industrial, domestic, and commercial loads grow rapidly, the demand for electricity on distribution feeders increases year after year. The growth in feeder load can be caused by either connecting new loads to the feeders or by increasing the usage of existing loads on the feeders. When the demand on the power feeder surpasses its capabilities, the feeder's ability to handle additional loads is restricted by voltage stability or thermal constraints. Before the feeder can accept any more loads, the voltage must be within acceptable parameters. Increased system load demands can lead to various negative consequences: (Mandefro, 2019): - increased power loss, increased cost of the feeder energy loss, increased cost of supplied energy, and voltage deviation.

To achieve a better voltage profile and lower power loss results, it is crucial to implement the mitigation techniques after developing the power loss minimization and voltage profile enhancement strategy. Various methods can be employed to decrease the loss and fluctuation of voltage in a distribution feeder. Some of the methods are discussed below (Amin et al., 2019; Taye, 2019):-

Conductor grading: This involves the replacement of the current feeder conductor with a superior, expertly crafted conductor to minimize resistance and maximize efficiency. One way to achieve this is by installing additional conductors that can work alongside the existing ones, or by replacing the current small-sized conductors with larger ones, by using conductors with a greater cross-sectional area, the resistance can be reduced effectively. While these approaches may lead to significant reductions in losses, they are not cost-effective. They are typically only employed under specific circumstances, as the expenses associated with purchasing and installing conductors outweigh the energy savings achieved(Taye, 2019).

Network reconfiguration: it is the art of manipulating switches to modify the circuit topology, all to reduce operating costs and fulfill predetermined requirements. Network reconfiguration could be utilized to reduce loss in distribution networks with a feeder arranged as a tree structure. This involves strategically opening or closing switches on the feeder to optimize the system's efficiency and minimize losses. By implementing network reconfiguration, loads can be efficiently transferred from overloaded feeders to less loaded ones. Additionally, transfers can also be made from higher resistance routes to lower resistance routes, resulting in the lowest overall loss. These transfers not only effectively adjust the loads on the switched feeder and reduce losses, but they also have a positive impact on the voltage profile along the feeder, as well as overall system power losses. Feeder reconfiguration may not be cost-effective for manual and spatially distant feeders (Abayneh & Fekadu Shewarega, 2022).

Using a High Voltage Distribution System: To decrease voltage fluctuation and distribution system loss, one effective approach is to implement a high voltage distribution system (Amin et al., 2019). This involves the strategic placement of high-voltage cables closer to the load, allowing for the use of smaller-rated transformers instead of large ones. Another option is upgrading existing low-voltage distribution network to high-voltage ones. By adopting these techniques, technical losses can be significantly reduced while enhancing power quality in distribution networks. It's worth noting that high-voltage devices operate with lower currents, which further contributes to efficiency. However, it is important to consider the initial investment required for such a system, as it may pose practical limitations.

Optimal Placement of DG: Distributed Generation (DG) is a cutting-edge approach in power systems that embraces the rising demand with unwavering support. Optimal placement of DG focuses on determining the most optimal positions and sizes for DG units, such as solar panels, wind turbines, etc., within a distribution network (Mehammed, 2017). By strategically placing DG units, they can efficiently cater to local power requirements and minimize the dependence on the primary grid. Consequently, this not only decreases power losses but also enhances the voltage profile. Nevertheless, determining the ideal locations for DG units entails an intricate optimization challenge (Iqbal et al., 2018). Factors ranging from network topology, load demand, and DG output, to operational restrictions need careful evaluation and consideration.

Reactive Power Compensation: this technique involves managing reactive power levels in an AC power system to enhance efficiency and system performance. One way to enhance the power system performance is through the application of a method that involves infusing reactive power into the network. This can be achieved by utilizing various tools, such as capacitors, reactors, and FACTS devices. By injecting reactive power, it becomes possible to enhance the voltage profile and counteract reactive power losses by mitigating the voltage drop along transmission lines (Abayneh & Fekadu Shewarega, 2022). However, it is important to exercise caution and maintain careful control over the application of reactive power injection to prevent detrimental issues like overvoltage or under voltage complications.

2.5. Distributed Generation (DG)

DG is a small-scale decentralized power generation technology which is connected to a distribution system to provide electrical energy at a site closer to the load centers than the central generation station. DG is a new technique based on non-renewable or renewable energy sources that can play a critical role in electrical power systems (Sarabia, 2011).

There are two broad categories of DG technologies depending on their sources: non-renewable and renewable, which as depicted in Figure 2.1. There are various distribution generation techniques in each category (Adefarati & Bansal, 2016; Getie & Dar, 2019).

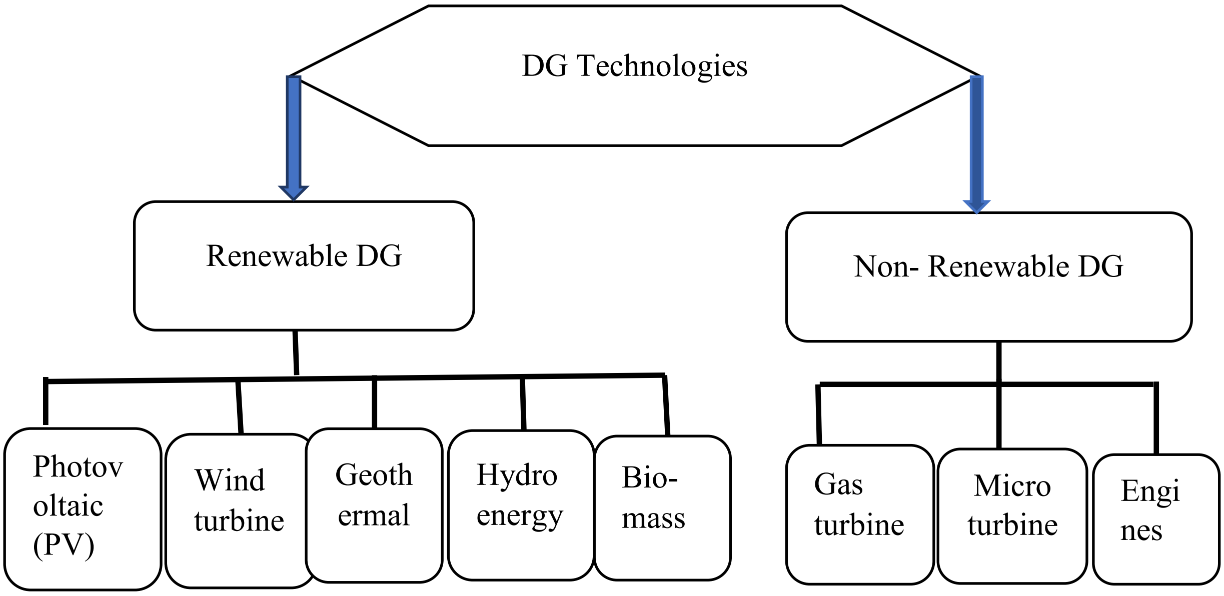

Figure 2.1: Types of DG Technologies

Again, based on their capabilities regarding active and reactive power injection, DGs can be categorized as follows, as outlined by (Yuvaraj & Ravi, 2018):

- Type I DG: This is a type of DG that injects only active power (P),
- Type II DG: This is a type of DG that injects both active (P) and reactive power (Q),
- Type III DG: This is a type of DG that injects active power into the grid, but it consumes reactive power from the grid.
- Type IV DG: This is a type of DG that injects only reactive power (Q),

A. Non-Renewable DG Technologies

Non-renewable DGs rely on fossil fuels, such as petroleum, coal, and natural gas, to generate energy for various applications. Unfortunately, these resources are not sustainable and cannot be replenished naturally. As the need for energy from non-renewable sources increases, and their rate of regeneration within the Earth remains fixed, they will eventually be depleted. Non-renewable energy sources can be harnessed using technologies such as gas turbines, reciprocating engines, micro-turbines, and steam turbines (Adefarati & Bansal, 2016).

Micro Turbine: A micro-turbine is a device that utilizes gas flow to convert thermal energy into mechanical energy (Mehammed, 2017). The core elements of the micro-turbine include a compressor, recuperator, combustor, turbine, and generator, and operates with the same principle as regular gas turbines. The air is sent into the compressor, where it is compressed and directed into the recuperator chilly side. There, it is preheated by the exhaust heat before entering the combustion chamber. In the combustion chamber, the warm air and fuel combine, which subsequently burns it. The mixture is expanded by the turbine, which powers the generator and compressor. Following that, the recuperator removes the burned air and the exhaust exit releases it. The voltage generated by micro-turbines is not compatible with the power grid or utility. Thus, conversion to DC and then back to AC is necessary to match the utility's standard voltage and frequency. The benefit of micro-turbines is their environmentally friendly operation with minimal emissions while maintaining good efficiency. However, they come with drawbacks such as high maintenance costs and a lack of extensive industry experience. Limited operational data is available due to the short operating periods of many micro-turbines, making it challenging to establish a robust database. Additionally, effective control and dispatch methods for many micro-turbines, as well as strategies for selling surplus energy, are yet to be fully developed.

B. Renewable DG Technologies

Fuel Cell: Fuel cells are electrochemical devices that, without the need for combustion, combine hydrogen as a fuel and oxygen as an oxidant to directly transfer chemical energy from a fuel into electrical energy (Abayneh & Fekadu Shewarega, 2022). Hydrogen is commonly extracted from natural gas, while oxygen is sourced from air. The outcome of this electrochemical device is DC power with high current and low voltage. To convert the fuel cell's DC output into AC power for the grid, a DC/AC converter and filter system are used.

These systems can be used as distributed generators, providing power in the range of a few kilowatts (kW) to 3 megawatts (MW) (Abayneh & Fekadu Shewarega, 2022). Fuel cells can efficiently convert fuels into electricity, achieving high efficiencies ranging from 35% to 60%, in comparison to conventional technologies. Due to the absence of combustion, emissions of harmful pollutants are minimal. The primary drawback of fuel cell commercialization is the substantial-high investment cost (Abayneh & Fekadu Shewarega, 2022).

Photovoltaic Systems: Photovoltaic systems transform the light energy harnessed from the sun into electrical energy (Mandefro, 2019. A photovoltaic (PV) system generates electricity using solid-state semiconductor devices that convert sunlight into electrical energy. A solar cell is the individual unit that forms a solar panel. A PV module comprises multiple solar panels interconnected in series or parallel. Solar panels are connected in series to maximize the output voltage and connected in parallel to maximize the output current. PV systems produce DC voltage, which is then converted to AC with the help of inverters to be integrated with the distribution network. These systems are environmentally friendly, releasing no harmful substances, featuring user-friendly and uncomplicated designs, and relying solely on sunlight as their fuel source. Both the surface area and the intensity of solar radiation impact the amount of current generated.

Wind Turbine: Wind turbines utilize the wind's kinetic energy to generate electrical power. Wind turbines are most effective in areas with high wind speeds, such as elevated regions and coastlines, where they can capture more kinetic energy for electricity generation. Like PV systems, wind turbines operate without fuel consumption and produce no emissions. Commonly the generator generates an AC voltage that fluctuates with the wind speed. Since wind speed is inherently variable, the generated voltage needs to be converted to DC and then back to AC using inverters. In contrast, no such conversion procedures are required for constant-speed wind turbines since they are connected directly to the grid (Mandefro, 2019). Wind energy faces challenges due to the variability of wind patterns, resulting in unpredictable electricity generation. Moreover, the initial investment costs associated with wind turbines are higher compared to photovoltaic (PV) systems, which harness solar energy (Taha, 2014). Wind speeds fluctuate throughout the day, leading to variations in power output. These fluctuations can affect power quality by causing fluctuations in voltage profile, increased power loss, and reduced voltage stability within the power system (Abayneh & Fekadu Shewarega, 2022).

2.5.1. Benefits of Distributed Generations (DG)

Renewable energy-driven distributed generation (DG) shows promising potential in current and future electricity generation. Its appeal lies in the incentives, adaptability, emission-free operation, and the recycling of energy resources, rendering distributed generation as the preferred energy source. Distributed generations have the following benefits:

Reduce electrical power loss: Integrating renewable DG units into the distribution system leads to a reduction of current flow within the feeders, thereby decreasing power loss. The impact of renewable distributed generation (DG) on power loss is influenced by factors like the size of the DG units, their placement, and the scale of the load.

Economic benefit: Renewable DG is positioned at or near load centers, the economic advantages of incorporating renewable DG can be realized by eliminating the need for investments in the distribution and transmission infrastructure. Incorporating DGs into the power system helps to reduce energy loss, resulting in lower energy costs. For a power plant to be optimally viable and financially sustainable, the cost of power generation must be lower than the selling price.

Additionally integrating distributed generation into the distribution system fulfills the load demand, enhances the voltage profile, increases the lifespan of system components, prevents network expansion, has environmental benefits, and enhances energy efficiency.

2.5.2. Applications of Distributed Generation (DG)

Typically, there are three key uses of DG (Mehammed, 2017). The primary application involves backup generation, where the DG unit stays offline during regular operation and is activated to provide power to loads in the event of an outage. Utilizing DG as a backup source enhances the reliability of the power supply, particularly for commercial and industry loads. This approach aids in enhancing the overall system reliability. DG can be employed to maintain a continuous power supply to specific load feeders through switch operations.

Another important application of DG involves its parallel operation with the main grid to assist loads, as well as to feed surplus power back into the grid when the DG capacity exceeds the demand from the feeder. During peak load periods, DG can provide support to the main grid when the feeder's capacity is insufficient to meet customer demand. And it reduces loss and interruption due to overload.

Another application is the DG can function independently to provide power to consumers who are not linked to the grid. For instance, it can be utilized as a standalone system in remote regions where the expenses associated with connecting to the main grid are prohibitively high.

In this work, DG is used as support for the main feeder line and, thereby reduces power losses. The effect of DG on distribution power loss is influenced by different factors such as the position and size of DG, switch operations, etc. However, in this thesis, the focus is on studying the optimal positioning and sizing of DG to streamline the complexity of the issue. The position and size of DG are critical in reducing power loss and maintaining voltage levels. Placing DG strategically can optimize these factors. The optimal sizing and placement of DG are explored in Chapter 3.

2.5.3. Type of DG Selected for the Research Area

There are different DG technology types, encompassing non-renewable and renewable sources, as elaborated in the preceding discussion. The selection criteria for DG technology resources in the specified study area are affected by various factors, including resource availability, land availability, cost, environmental conditions, community willingness, infrastructure like road access for material transport and maintenance personnel, and more.

PV system was chosen in this thesis for the study area, due to the following factors (Taha, 2014) (Mehammed, 2017):-

Environmental Condition: Solar energy serves as an eco-friendly electricity generation system that is clean, emits low level of pollutants, thereby reducing greenhouse gas emissions and mitigating acidification.

Resource Availability: The sole essential resource needed is sunlight and solar radiation, which represents the quantity of sunlight reaching the surface each day in KWh/m²/day. This key value is crucial for selecting the appropriate site and technology for the specific area. Solar energy production is viable in nearly all regions of Ethiopia due to its proximity to the equator. In Adama, the yearly average solar radiation received on a horizontal surface amounts to 6.16 kWh/m²/day as discussed in Chapter Three section 3.5.

Cost: While the initial setup expenses are considerable, the maintenance and operational costs are minimal, with almost negligible ongoing expenses. The operation and maintenance costs could be:

- **Administration maintenance:** Creating financial plans and obtaining funding for preventive maintenance, liaising with clients, maintaining records, reporting on system efficiency, and evaluating the effectiveness of the operations and maintenance (O&M) program.
- **Preventative maintenance:** Arranging maintenance inspections in accordance with manufacturer guidelines to adhere to equipment warranties. The frequency of preventive maintenance is established based on the equipment type, environmental factors, and the terms outlined in the warranties.
- **Corrective maintenance**: Necessary to address repairs or replace malfunctioning components. Non-critical corrective maintenance activities can be combined with scheduled preventive maintenance activities.
- **Condition-based maintenance**: Utilizing data loggers to access real-time data for planning preventive actions such as cleaning tasks. Predicting potential failures in advance or detecting them at an early stage.

Usage time: The time that a technology or product can function effectively at a desired level of efficiency is known as its usage time. The product's life characteristics, including time-to-failure (TTF), are typically determined using actual field data on degradation. For photovoltaic (PV) systems, the end of their useful life is frequently predicted by linearly extrapolating based on the system's annual degradation rate in practical use. This estimation usually involves reaching a 20% decrease from the rated power output, which falls within the range of a 0.5% to 0.8% maximum decline each year. In this thesis, a lifespan of 25 years is assumed for the PVDG system (IRENA, 2019).

2.5.4. Mathematical Modelling and Components of PV System

Mathematical Modelling of PV Cell

Figure 2.2 shows a solar cell equivalent circuit (Kongming Sun et al., 2020) featuring four distinct electrical components with easily understandable behaviors. Within the equivalent circuit, λ symbolizes the illumination intensity, while I_{PV} depends onλ, solar cell area, and temperature, which denotes the photogenerated current. I_d stands for the combined diffusion current flowing across the pn-junction.

An ideal solar cell is typically modeled by only a current source in a shunt with a diode. But in the case of practical solar cell modeling additional elements like the shunt resistor Rp and series resistor Rs are incorporated into the circuit (Kongming Sun et al., 2020). Rs accounts for losses arising from inadequate conductivity and poor external connections, whereas Rp pertains to losses resulting from imperfect rectifying devices, involving current leakage through the cell and along its edges. Typically, Rp tends to have a significantly high value, whereas Rs is very small, making both values insignificant when the cell is idealized.

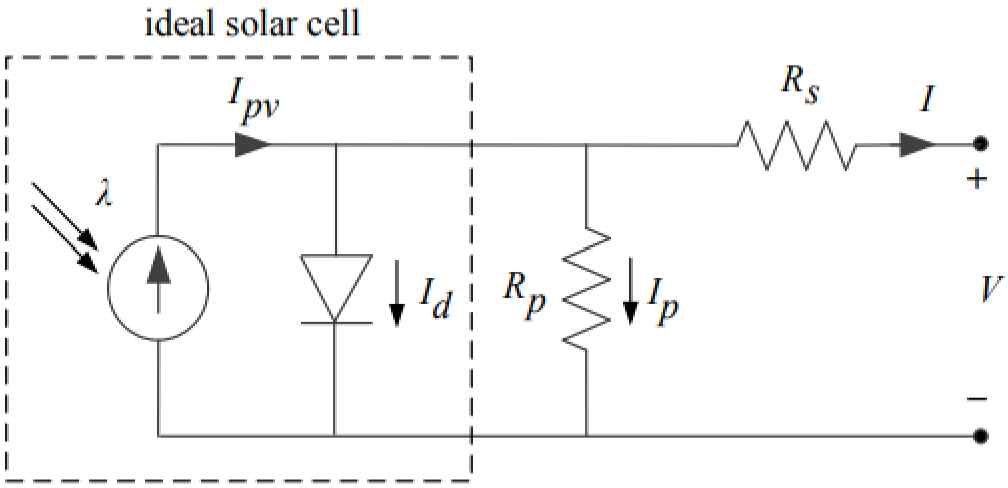

Figure 2.2: The equivalent circuit of solar cell (Kongming Sun et al., 2020)

The mathematical representation of a PV cell is derived from its equivalent circuit. The current generated by the solar cell is the sum of the current flowing through the diode (Id) and the current flowing through the shunt resistor (Ip), subtracted from the current produced by the current source.

$$I = I_{PV} - (I_d + I_p) \qquad (2.1)$$

The voltage drop across the diode is given by: -

$$V_d = V + IR_S \qquad (2.1)$$

This voltage is equal to the voltage across the shunt resistor. The current through the diode is calculated as:

$$I_d = I_o\{e^{\frac{qV_d}{\alpha kT}} - 1\} \qquad (2.3)$$

Where I_o is the reverse saturation current when the illumination intensity is zero,

q is the elementary charge ($1.6x10^{-19}$C),

α is ideality factor (1 for an ideal diode), k is Boltzmann's constant ($1.38x10^{-23}$J/K),

T is the absolute temperature.

The current through the shunt resistor is given by: -

$$I_p = \frac{V_d}{R_p} \tag{2.4}$$

Now, by substituting Equation (2.2) into Equation (2.4) we will get:-

$$I_p = \frac{V + IR_S}{R_p} \tag{2.5}$$

Finally, by substituting Equations (2.2), (2.3), and (2.5) into Equation (2.1) we will get:-

$$I = I_{PV} - I_o\{e^{\frac{qV_d}{akT}} - 1\} - \frac{V + IR_S}{R_p} \tag{2.6}$$

Component of PV System

A standard solar PV setup includes components like solar panels, a charge controller, batteries, an inverter, and the distribution bus bar. The block diagram below illustrates the configuration of such a system.

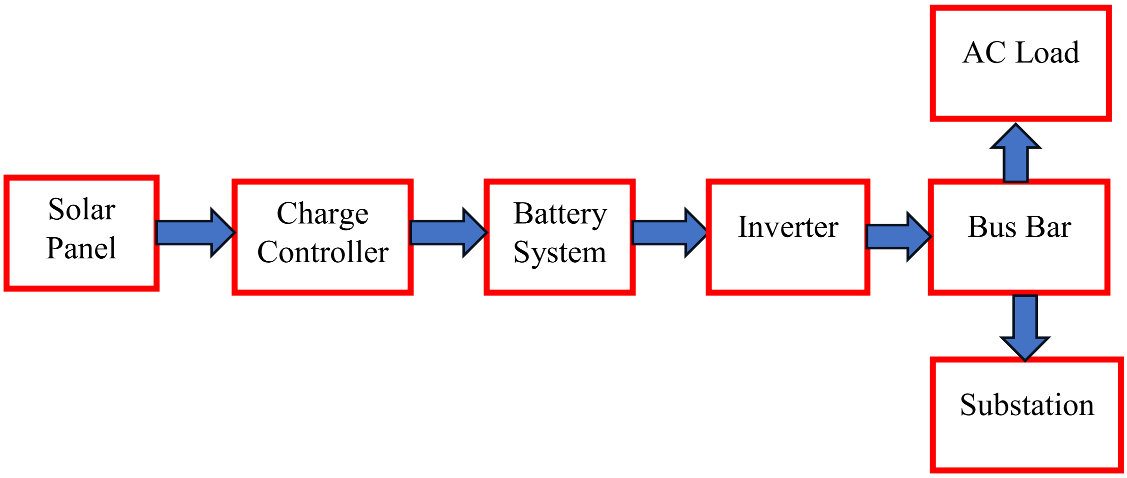

Figure 2.3: Block Diagram of PV System (Kaushal & Basak, 2019)

The above block diagram shows a setup capable of both providing power and storing it. During peak demand, the system feeds energy from the inverter to the bus bar and subsequently to the load. When there's less need for electricity, the battery can store excess energy generated by the solar panel. The charge controller controls this stored energy. It acts as a backup power source to make sure that there is electricity available during overcast days or at night when the solar panel is not producing electricity.

Solar Panel

Solar panels of various kinds are utilized to transform solar energy into electrical power. Each panel is composed of numerous individual solar cells. Solar cells are constructed using layers of silicon (serving as a semiconductor), phosphorus (negative charge), and boron (positive charge). Similarly, sunlight comprises diverse energy particles referred to as "photons." When photons interact with the surface of solar panels, they dislodge electrons from silicon, initiating a specific electric current that travels through silver busbars and fingers embedded on the silicon cells. This is how solar panels generate energy, a process referred to as the Photovoltaic Effect. Different types of solar panels are there, some of them are: - Mono-crystalline, Amorphous Silicon, Polycrystalline, and Thin film solar cells (Mehammed, 2017).

Charge Controller

The inclusion of a battery in a system highlights the need for a charge controller (Mehammed, 2017). Usually, the controller's primary function is to ensure the batteries receive proper charging, thereby ensuring their long-term safety and usability. During a bright sunny day, the solar cells may generate excessive voltage, potentially causing harm to the battery. Subsequently, the charge controller prevents overcharging by limiting the energy flow to the battery once it hits a specific voltage threshold. Furthermore, charge controllers are used to stop the battery from discharging back into the solar panels during night time.

Batteries

Batteries can be used to store charges. A battery consists of two electrodes submerged in a liquid called an electrolyte. This electrolyte allows ions to flow between the electrodes, which is essential for conducting electricity. Recent advancements have led to ongoing enhancements in battery safety, dependability, effectiveness, efficiency, affordability, and storage capacity. There are four types of battery technologies utilized in power applications (Mesgana Tulu, 2023): - Nickel-cadmium, lead-acid, Flow batteries, and lithium-ion.

The lead-acid battery stands as an economical and well-established energy storage solution. Nevertheless, it faces challenges in multiple areas including low energy density (50-80 kWh/m^3), limited power density (90-700 kW/m^3), shortened lifespan (250-1500 cycles), frequent maintenance, and the utilization of toxic materials. However, the lithium-ion battery features high energy density (1300-10000 kWh/m³) and power density (300-750 kW/m³), an extended lifespan (500-10000 cycles), fast response time, minimal memory effect, and recyclability. While Li-ion batteries come at a higher cost than lead-acid batteries, they are capable of accommodating higher C-rates compared to lead-acid batteries. Nickel-cadmium batteries exhibit durability and can function in extreme temperature conditions. They eliminate the need for sophisticated battery management systems and are essentially maintenance-free.

2.6. Flexible AC Transmission Systems (FACTS) Devices

FACTS devices are power-electronic devices and other static controllers used in AC power transmission systems. They improve controllability and boost power transmission capacity by managing voltage, current, and power flow (Hingorani et al., 2000). FACTS devices are designed with cutting-edge power electronics technology and possess the capability to execute control actions at a high speed. The primary function of FACTS is to control power flow and regulate voltage levels in the transmission lines where they are connected. FACTS devices can be classified into two based on the power electronics devices they use; Thyristor valve/convertor-based FACTS devices like TCSR, TCSC, and SVC and voltage source convertor-based FACTS devices such as STATCOM, SSSC, and UPFC.

In general FACTS devices can be classified as below (Hingorani et al., 2000).

- Shunt connected controllers like SVC, STATCOM, etc.
- Series-connected controllers like SSSC, TCSR, etc.
- A combination of series-connected and shunt connected controllers like UPFC and TCPST.

A) Shunt Connected Controllers

Shunt connected controllers are employed to inject the current into the line. By ensuring that this injected current is in quadrature (90 degrees out of phase) with the line voltage, the shunt controller can supply reactive power without affecting the flow of active power. In cases where the injected current is not in quadrature phase, actual power is utilized. SVC and STATCOM, are the two examples of shunt connected controllers.

i) Static Var Compensator (SVC):

A shunt connected SVC is a device that can be fine-tuned to either inject or absorb reactive power into the electrical grid. This adjustment capability allows for the regulation of specific parameters within the power system, such as maintaining desired voltage levels at specific points (buses) in the network (Hingorani et al., 2000). SVC is constructed using thyristors that do not possess a gate turn-off feature. It consists of individual components for managing lagging and leading Vars: a thyristor-controlled reactor to absorb reactive power and a thyristor-switched capacitor for delivering reactive power. The simplicity, minimal losses, reduced harmonics generation, and cost-effectiveness of SVC have led to its extensive utilization in comparison to other shunt FACTS devices (Abayneh & Fekadu Shewarega, 2022).

ii) Static Synchronous Compensator (STATCOM)

STATCOM functions as a shunt connected SVC, enabling independent control of its capacitive or inductive output current regardless of the AC system voltage (Hingorani et al., 2000). STATCOM is an essential FACTS controller that can be implemented using either a voltage-sourced converter or a current-sourced converter. From a cost perspective, voltage-sourced converters appear to be the preferred choice (Hingorani et al., 2000). It adjusts the system's active and reactive power through the conversion of DC input voltage to AC output voltage. STATCOM is employed in the mechanism of voltage regulation and reactive power compensation, with superior performance compared to SVC. STATCOM enhances power system stability, mitigates power oscillations in transmission systems, and ensures adequate reactive power compensation. It achieves this by regulating voltage levels within transmission and distribution networks. When a STATCOM incorporates an energy storage system at its DC terminal, it can exchange real power with the system (Abayneh & Fekadu Shewarega, 2022).

The key distinction between an SVC and a STATCOM lies in their operational methods. A STATCOM employs a converter to generate reactive power and operates like a shunt-connected synchronous voltage source. On the other hand, an SVC utilizes Thyristor-switched capacitors and, Thyristor-controlled reactors, operating as a shunt-connected controlled reactive admittance.

B) Series Connected Controllers

In operation, all series controllers introduce voltage along with the line. This includes cases where a variable impedance interacts with the current passing through it generates a series voltage along the line (Hingorani et al., 2000). Only reactive power is exchanged by the series controller when the line current and the voltage are in phase quadrature. However, if the current and voltage are not in quadrature, the controller will be involved in handling real power.

i) Static Synchronous Series Compensator (SSSC)

SSSC is one of the most significant FACTS controllers. It operates similarly to a STATCOM but differs because its alternating current (AC) voltage output is connected in series with the transmission line. SSSCs can utilize either voltage-sourced converters or current-sourced converters. DC bus (storage unit), converter, and coupling transformer make up the SSSC (Abayneh & Fekadu Shewarega, 2022). Typically, the voltage injected in series is significantly lower than the voltage of the transmission line (Hingorani et al., 2000). Reactive power is transmitted when the injected voltage is in quadrature with the line current; active power is exchanged when the injected voltage is in phase with the line current. Therefore, the STATCOM has the capability to exchange both real and reactive power within a transmission line when it's with energy storage (Abayneh & Fekadu Shewarega, 2022).

ii) Thyristor-Controlled Series Capacitor (TCSC)

It's a compensator with capacitive reactance comprising a series capacitor bank, and shunted thyristor-controlled reactor to offer a smoothly adjustable series capacitive reactance (Hingorani et al., 2000). The TCSC utilizes thyristors that do not have a gate turn-off feature. It serves as an option to the SSSC mentioned earlier and, similar to the SSSC, it holds significant importance as a FACTS controller. A variable reactor like a Thyristor-Controlled Reactor (TCR) links with a series capacitor. When the TCR firing angle hits 180 degrees, the reactor goes non-conductive, allowing the series capacitor to exhibit its usual impedance. Conversely, when the TCR firing angle hits 90 degrees, the reactor transitions into full conduction, causing the overall impedance to become inductive. This shift occurs as the reactor impedance is intentionally set lower than that of the series capacitor impedance. Operating at a 90-degree firing angle, the TCSC plays a role in limiting fault current. TCSC can exist as either a single large unit or as multiple capacitors of equal or varying sizes to enhance its efficiency.

C) Combination of Series and Shunt-connected Controllers

This scenario could involve a mix of distinct shunt and series controllers, operated in a synchronized fashion, or a Unified Power Flow Controller integrating both series and shunt elements (Hingorani et al., 2000). In general, shunt and series controllers are combined to introduce current into the system using the shunt component of the controller and insert voltage in series with the line through the series portion of the controller. Yet, in the case of integrated shunt and series controllers, an exchange of real power can occur between the series and shunt controllers via the power link (Hingorani et al., 2000).

i) Unified Power Flow Controller (UPFC)

UPFC is set up comprising STATCOM and SSSC, coupled through a shared DC link, which enables bidirectional real power exchange between the output terminals of the SSSC and the STATCOM. This configuration is to deliver simultaneous actual and reactive power, series compensation without necessitating an external electrical power source (Hingorani et al., 2000). The UPFC is capable of simultaneously adjusting all three aspects of line power flow; voltage, line impedance, and phase angle (Abayneh & Fekadu Shewarega, 2022). The SSSC unit acquires its active power from the line through the associated STATCOM shunt unit, which also serves as a voltage regulator by managing its reactive power. This comprehensive controller manages both actual and reactive power distribution across the line, while also maintaining control over line voltage. Incorporating extra storage like a superconducting magnet linked to the DC link through an electronic interface would offer a way to boost the effectiveness of the UPFC even further (Hingorani et al., 2000).

ii) Thyristor-Controlled Phase Shifting Transformer (TCPST)

A phase-shifting transformer, controlled using thyristor switches, to deliver a quickly adjustable phase angle. Typically, phase shifting is achieved by introducing a perpendicular voltage vector in conjunction with a phase in series. This vector is generated from the remaining two phases through transformers connected in parallel (Hingorani et al., 2000). The adjustable perpendicular series voltage is achieved through various power electronics setups. A circuit design capable of managing voltage reversals can induce phase shifts in either direction.

Overall, the effectiveness of FACTS devices across various uses is summarized in Table 2.1(Hingorani et al., 2000; Abayneh & Fekadu Shewarega, 2022).

Table 2.1: Summary of FACTS device applications

FACTS Devices					
Connection type	Series		Shunt		Combined
Device	TCSC	SSSC	SVC	STATCOM	UPFC
Problem					
Dynamic voltage control	***	**	**	**	***
Steady-state phase balancing	*	*	**	**	***
Steady-state voltage control	***	**	**	***	***
Steady-state power flow control	**	**	***	***	***
Transient stability	**	*	***	**	**

***, Strong influence; **, Medium influence; *, Low influence

2.6.1. Distribution Static Synchronous Compensator (DSTATCOM)

STATCOM (Static Synchronous Compensator) is a shunt-connected FACTS device that helps to control the flow of electricity in high-voltage transmission networks. It is referred to as DSTATCOM when utilized in a low-voltage distribution network. DSTATCOM is a three-phase shunt-connected FACTS device implemented based on a voltage source converter (VSC) to compensate reactive power and to enhance the voltage profile in the distribution system. The DSTATCOM may inject or absorb both actual and reactive power at the point of common connection (PCC). However, it is practically unfeasible for DSTATCOM to inject active power continuously for an extended duration due to the limitations imposed by energy storage. Therefore, most of the time in steady state operation there is only reactive power exchange between DSTATCOM and the system. The common type of DSTATCOM designed for steady-state operation includes a transformer with leakage reactance, a DC capacitor, a voltage source converter (VSC), and a GTO/IGBT in its configuration (Iqbal et al., 2018). Figure 2.4 shows a schematic diagram of DSTATCOM connected to a bus k (Abayneh & Fekadu Shewarega, 2022)

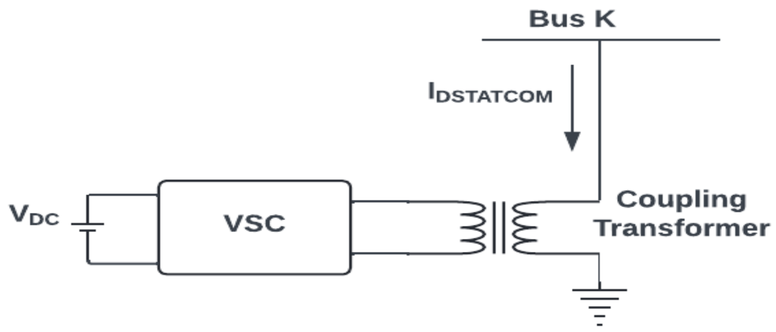

Figure 2.4: DSTATCOM connected to a certain bus k

The DSTATCOM controls reactive power exchange by adjusting the amplitude of its output voltage, which is synchronized with the system voltage (Vs). When the DSTATCOM output voltage (Vsc) is higher than Vs, it injects reactive power into the system, acting as a capacitor (capacitive mode). Conversely, when Vs is higher than Vsc, the DSTATCOM absorbs reactive power, acting as an inductor (inductive mode). When Vsc equals Vs, no reactive power exchange occurs, resulting in a zero net reactive power flow (no-load mode) (Hingorani et al., 2000).

2.6.1.1. Mathematical Modelling of DSTATCOM

This section presents the mathematical modeling of DSTATCOM. Most of the time, distribution networks are designed in a radial manner, in which power is supplied from one side only. The mathematical modeling of DSTATCOM in a steady state can be illustrated using a basic distribution network with two buses, as depicted below.

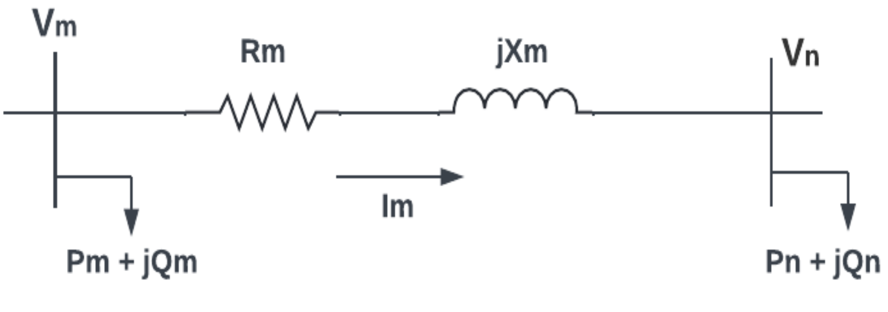

Figure 2.5: Two-bus radial distribution network

Where R_m denotes the line resistance and X_m denotes the line reactance between the bus m and n, $P_m + jQ_m$ and $P_n + jQ_n$ denote the local loads connected at the bus m and n, respectively. Likewise, V_m and V_n, denote the voltages at the bus m and n, respectively.

The voltage equation for a two-bus system can be expressed as:

$$V_n = V_m\angle\theta_m - (R_m + jX_m)I_m\angle\delta \quad (2.7)$$

The DSTATCOM is installed at two bus radial distribution networks for steady-state modeling, as depicted in Figure 2.6.

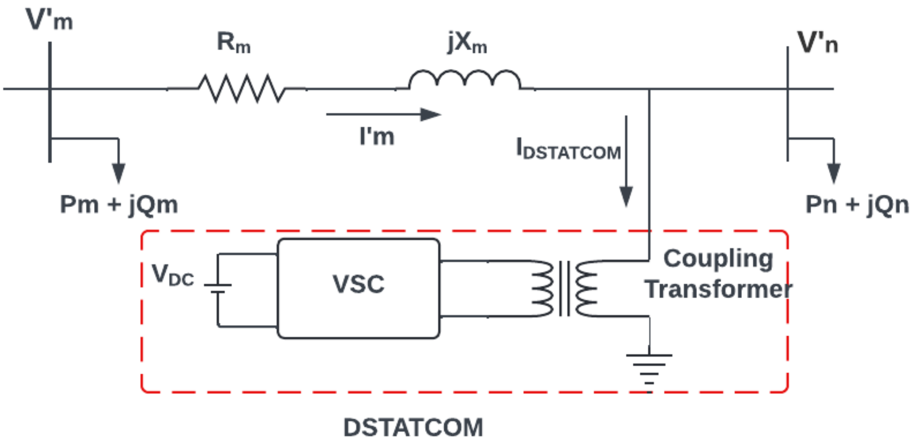

Figure 2.6: Two-bus radial distribution network with DSTATCOM

After the installation of DSTATCOM, the voltages at the bus where it's connected and at the neighboring bus will change. The new voltage values at the candidate bus will be denoted as V'_n and at the previous neighboring buses as V'_m. These changes in voltage are accompanied by changes in the current, denoted as I'_m. The new current is a combination of I_m and I_{DSTATCOM}, where I_{DSTATCOM} represents the current injected by DSTATCOM. Consequently, the expression for the new voltage after installing DSTATCOM can be formulated as follows.

$$V'_n\angle\theta'_n = V'_m\angle\theta'_m - (R_m + jX_m)(I_m\angle\delta + I_{\text{DSTATCOM}}\angle(\tfrac{\pi}{2} + \theta'_n)) \quad (2.8)$$

Where θ'_n, $\theta'_{m,}$ and δ are the phase angles of V'_n , V'_m and I_m respectively.

Once we separate the real and imaginary parts of the previous equations, we get:

$$V'_n cos\theta'_n = Real(V'_m\angle\theta'_m) - Real(Z_m\, I_m\angle\delta) - R_m I_{\text{DSTATCOM}} cos\left(\frac{\pi}{2} + \theta'_n\right) + X_m I_{\text{DSTATCOM}} \sin(\tfrac{\pi}{2} + \theta'_n) \quad (2.9)$$

$$V'_n sin\theta'_n = Imag(V'_m\angle\theta'_m) - Imag(Z_m\, I_m\angle\delta) - X_m I_{\text{DSTATCOM}} cos\left(\frac{\pi}{2} + \theta'_n\right) - R_m I_{\text{DSTATCOM}} \sin(\tfrac{\pi}{2} + \theta'_n) \quad (2.10)$$

Let us use the following assumptions:

$d = V'_n$

$b_1 = Real(V'_m \angle \theta'_m) - Real(Z_m\, I_m \angle \delta)$

$b_2 = Imag(V'_m \angle \theta'_m) - Imag(Z_m\, I_m \angle \delta)$

$b_3 = X_m$

$b_4 = R_m$

$x_1 = I_{DSTATCOM}$

$x_2 = \theta'_n$

Then, Equations (2.9) and (2.10) are rewritten as:

$$dcosx_2 = b_1 + b_4x_1sinx_2 + b_3x_1cosx_2 \tag{2.11}$$

$$dsinx_2 = b_2 + b_3x_1sinx_2 + b_4x_1cosx_2 \tag{2.12}$$

Then from Equations (2.11) and (2.12), we have

$$x_1 = \frac{dcosx_2 - b_1}{b_4sinx_2 + b_3cosx_2} \tag{2.13}$$

$$x_2 = \frac{dsinx_2 - b_2}{b_3sinx_2 + b_4cosx_2} \tag{2.14}$$

Now by equating Equations (2.13) and (2.14) by taking t = $sinx_2$ we will get:

$$(K_1^2 + K_2^2)t^2 - (2K_1db_4)t + (d^2b_4^2 - K_2^2) = 0 \tag{2.15}$$

Where $K_1 = b_1b_3 - b_2b_4$ and $K_2 = b_1b_4 - b_2b_3$

The solution of the Equation (2.15) can be written as:

$$t = \frac{2K_1db_4 \pm \sqrt{(2K_1db_4)^2 - 4(K_1^2 + K_2^2)(d^2b_4^2 - K_2^2)}}{2(K_1^2 + K_2^2)} \tag{2.16}$$

$$\theta'_n = x_2 = \sin^{-1}t \tag{2.17}$$

The injected voltage, current, and reactive power at bus n, will be given as follows:

$$V'_n = V'_n \angle \theta'_n \tag{2.18}$$

$$i_{DSTATCOM} = i_{DSTATCOM} \angle (\theta'_n + \frac{\pi}{2}) \tag{2.19}$$

$$jq_{DSTATCOM} = V'_n i^*_{DSTATCOM} \quad (2.20)$$

Figure 2.7 below illustrates the phasor diagram depicting the two-bus system with DSTATCOM.

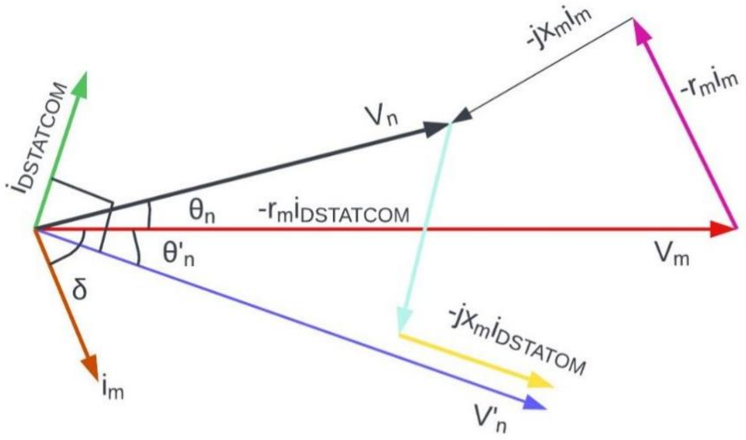

Figure 2.7: The voltage and current phasor diagram of the system after taking DSTATCOM into account

2.6.1.2. Reason for Choosing DSTATCOM

A critical system limitation in the distribution network involves meeting the entire load's power requirements while maintaining the voltage magnitude within a permissible range. To address this challenge, it requires the implementation of advanced technologies to maintain voltage levels within the acceptable range and to reduce power losses in the distribution system. Examples of such devices include shunt and series reactors, capacitor banks, automated voltage regulators (AVRs), as well as FACTS devices like the SVC, DSTATCOM, UPQC, and SSSC. DSTATOM may supply or absorb reactive power continuously and quickly.

When the DSTATCOM is connected to a particular load, it can deliver sufficient leading or lagging compensating current to guarantee that the total demand meets the utility connection standards. At the same time, it has the capability to eliminate any voltage imbalance or harmonic distortion. Optimal placement of DSTATCOM enhances load capacity, decreases power losses, stabilizes the system, provides reactive power support, and improves power quality.

DSTATCOM offers various benefits in comparison to traditional reactive power compensation devices, such as reduced power losses, minimal harmonic emissions, superior control features, cost-effectiveness, and compact dimensions. Furthermore, unlike shunt or series capacitors, DSTATCOM does not face operational challenges like resonance or transient harmonics.

In summary, DSTATCOM has the following basic functions:

- Increases the loading capacity of the distribution system.
- Reduce power losses
- Voltage regulation and reactive power compensation
- Reduce harmonic currents
- Voltage flicker mitigation
- Power factor correction

2.7. Literature Review

Several methods have been proposed by different researchers to address the issue of voltage drop and power loss in distribution networks. Some of them are discussed below.

The authors (Devabalaji & Ravi, 2016) proposed an innovative technique for finding the best locations and sizes of DG and DSTATCOM while formulating an objective function to reduce operational costs and power loss and improve the system's voltage profile. LSF was employed to find the optimal place of DG and DSTATCOM, while BFOA was used to find the appropriate size of DG and DSTATCOM.

In (Amin et al., 2019) the author, proposed an analytical method for optimal sizing and placement of DG and DSTATCOM in RDS to reduce the total power loss and enhance the voltage profile. The optimal place of DG and DSTATCOM was identified using PSI, while sensitivity analysis was utilized to find the optimal sizes of DG and DSTATCOM. The suggested algorithm effectiveness and performance have been validated using the IEEE 34-bus and IEEE 69-bus RDS, and the results have been compared to other methods.

This paper (Aditya Prasad Padhy, 2020) contributes an analytical method to find the optimal size and location of DGs for RDS. Comparing the proposed technique to other methods, it is computationally faster. Enhancing voltage profiles and minimizing an overall active power loss was the main objective of this work. In this work, VSI was employed to identify the loaded bus in the system. The bus with the highest load was chosen as the best place for the DG placement. The continuous increment of step size (CISS) technique was used to find the size of the DG at the identified location.

In (Lasmari et al., 2020) the author proposed various PSO algorithms to solve the problem of optimal simultaneous integration of the PV-based DG and DSTATCOM units in the standard IEEE 33-bus and 69-bus EDSs. The optimization considers a single objective function and aims to maximize APLL for the best optimal EMS.

In (Bilgundi, 2020), the author introduced an analytical method to find the best location and capacity of DG and DSTATCOM to reduce active power losses and enhance the voltage profile. The research utilized the PSI method to determine the best location and capacity for DGs and DSTATCOM in the distribution systems. The study utilizes BFS load flow analysis for its investigation. The validity of the analytic method is confirmed by applying it to the IEEE-33 bus system with single DSTATCOM, and single and multiple DG units. The programming is carried out using MATLAB software.

In (Salkuti, 2021), the author proposed a methodology to find the optimal size and location of DSTATCOM and DG to reduce power loss and enhance the voltage profile in RDSs. The study, utilized VSI to find the optimal place of DSTATCOM, while LSF to find the optimal place of DG and Bat algorithm (BA) was utilized to determine the optimal size of both DG and DSTATCOM in RDSs. The effectiveness of the suggested optimization problem was evaluated by applying it to standard IEEE 34 bus and 85 bus RDS. Finally, the author concluded that the simultaneous placement of DG and DSTATCOM devices in RDSs minimizes power loss and enhances the voltage profile.

In (Alwazni & Al-kubragyi, 2021) the author, proposed a MOPSO to find the optimal place and sizing of DG and DSTATCOM. The main objective function of this paper is to enhance the voltage profile, and voltage stability and reduce the total power loss of the RDS. The optimal placement of DG and DSTATCOM is pre-determined using VSI. Then MOPSO is employed to determine the capacity of DG and DSTATCOM units with various load models. Finally, the author concludes that the optimal placement of DG and DSTATCOM with MOPSO improves the voltage profile, and voltage stability and minimizes the total power loss of the distribution network more effectively than other optimization techniques in various scenarios.

In (Reddy et al., 2022) the author proposed FLFBA to find the optimal position of DG and FACTS devices in the distribution system. The objective was to enhance the minimum VSI of the distribution network. The analysis also considered minimum active and reactive power losses. The technique was evaluated by applying it to standard IEEE 33 distributed test systems and it was compared with other optimization algorithms such as firefly algorithm (FA), BA, and PSO algorithm. Finally, the author concluded that implementing DG and FACTS devices in the distribution system using FLFBA is effective. The author also suggests that this algorithm can be employed to solve different optimization problems.

In (Mustapha et al., 2023) the authors examined the ABC-based optimal positioning of DG and DSTATCOM considering various load factors in RDS, and minimization of real and reactive power loss and enhancement of voltage profile is the objective function. The study compared the effectiveness of placing these compensating devices at the same location versus separate locations. According to the results, placing the DSTATCOM and DG at different places reduces overall power loss more than placing them at the same place. Furthermore, placing them optimally at different locations obtained greater performance with lower compensator ratings. However, placing DG and DSTATCOM at the same place led to a slight enhancement in the voltage profile.

In (Maurya & Sharma, 2023) the author developed an AOA to obtain the optimal place and size of DGs and DSTATCOM in RDS. The objective of the study is to reduce power loss, and voltage deviation while improving VSI, and annual energy saving, all within the constraints of the system. DGs were employed to compensate active power, whereas DSTATCOM was used to compensate reactive power. Finally, through simulation, the authors illustrated that the simultaneous placement of DG and DSTATCOM reduces power losses, and enhances voltage profile and VSI in RDS. Furthermore, the suggested AOA performed better when compared to the BFOA, Grasshopper, and Immune algorithms.

In (Ferminus Raj & Gnana Saravanan, 2023) the author proposed a hybrid approach of LSF and DMO to obtain the optimal place and size of DG and DSTATCOM to minimize the power loss, improve the voltage profile, and minimize the operation cost. The authors have employed LSF to obtain the primary locations of DG and DSTATCOM and then used DMO to find the optimal size and final locations of these devices. To validate the proposed system, the authors conduct simulations using MATLAB Simulink and assess its dynamic stability performance with IEEE standard benchmark systems. The proposed method's simulation results are contrasted with existing techniques like DA, SGO, and SAA.

This manuscript (Isha et al., 2023) proposed a new algorithm called Elitist Harris Hawks Optimization (EHHO), for solving the multi-objective function by optimal placement and sizing of PV and DSTATCOM in RDS. Power loss reduction, voltage stability, and voltage profile enhancement are included in the multi-objective function. The optimal place and size of DG and DSTATCOM are determined by using the suggested EHHO algorithm. The Newton-Raphson method is employed to analyze the load flow. The performance of the recommended method is demonstrated on the standard IEEE-30 bus network. For simulation, MATLAB software is used. The results were compared to other techniques such as FLSA, IWHO, TLBO, and BONMIN under different load conditions, and it was observed that the EHHO algorithm performs better than the existing techniques.

Table 2.2: Sample of literature review

S/N.	**Title of Journals**	**Year of publi.**	**Gaps**
1	Optimal placement and sizing of DG and DSTATCOM in a Radial Distributed Systems Based on Analytical Technique (Bilgundi, 2020).	2020	• PSI technique is used to find both location & size. • BFS is used for load flow analysis. • DG type is not mentioned.
2	Optimal Allocation of DG and D-STATCOM in a Distribution System using Evolutionary-based BA (Salkuti, 2021).	2021	• Sensitivity techniques is used to find the location. • BA is used to find the size. • Single Objective function(APL) is used.
3	Enhancement of an Iraqi Radial Distribution System Performance Using Multi-Object Particle Swarm Optimization In (Alwazni & Al-kubragyi, 2021).	2021	• VSI is used to determine the location. • Newton-Raphson is used for load flow. • DG type is not mentioned. • No Installation cost estimation.
4	An optimization approach for optimal location and size of DSTATCOM and DG (Ferminus Raj & Gnana Saravanan, 2023).	2023	• LSF is used to determine the placement. • DMO is used to determine the size. • DG type is not mentioned.

			• No Installation cost estimation.
5	Elitist Harris Hawks Optimized Voltage Stability Enhancement in Radial Distribution System ((Isha et al., 2023).	2023	• EHHO is used determine both placement and size. • Newton-Raphson is used for load flow. • No Installation cost estimation.

In general, the literature review in this section discusses the minimization of power loss and enhancement of the voltage profile through optimal placement and sizing of DG and DSTATCOM using various optimization techniques. Most of the earlier studies used analytical methods to find the optimal place of DG and DSTATCOM. Some of them used a single objective function to determine both the size and location of DG and DSTATCOM. Some of them used Newton Raphson method to analyze load flow. And again, most of them did not do the investment cost analysis of DG and DSTATCOM. This study fills the gap of earlier studies in the area of optimal positioning and sizing of DG and DSTATCOM such as using metaheuristic optimization algorithms for placement and sizing, multi-objective optimization functions, direct load flow analysis techniques, and analyzing the investment cost. Furthermore, the integration of DG and DSTATCOM in a distribution system for power loss reduction and voltage profile enhancement has been studied.

CHAPTER THREE

3. MATERIALS AND METHODS

3.1. Introduction

This chapter focuses on, the optimal positioning of DG and DSTATCOM devices to enhance the performance of distribution systems. Accordingly, section 3.2 describe geographic description of the study area, section 3.3 presents about data collection, section 3.4 discusses the impedance calculation of the overhead line, section 3.5 discusses about the solar radiation of Adama city, section 3.6 discusses the load flow analysis, section 5.7 presents incorporating DG and DSTATCOM into load flow analysis, section 3.8 discusses problem formulation, section 3.9 presents the proposed method for the optimal sizing and positioning of DG and DSTATCOM, finally, section 3.10 presents the PSO algorithm with optimal positioning and sizing of DG and DSTATCOM.

3.2. Description of Case Study Area

Adama substation II is found in the east part of Ethiopia, located in the Oromia region east Shoa zone nearest to Adama city. Adama substation II is far away from Addis Ababa at a distance of around 120 km and found at a location of 8°35'13.3"N 39°18'37.6"E.

3.3. Data Collection

The data essential for this research has been gathered from the Adama distribution substation II, the load dispatch center, as well as Ethiopian Electric Power (EEP), Ethiopian Electric Utility (EEU), Ethiopian National Metrology, and NASA. The data was collected from historical records of feeder loading (peak load) at the substation, solar radiation, and other significant datasets.

In Adama City, there are two distribution substations namely Adama substation I and Adama substation II. Adama substation I, has three 132 KV incoming lines from Koka, Awash, and Adama-I Wind Firm. There are three stepdown transformers (132/15 KV), two of them are a winding transformer with a capacity of 25 MVA, which operate in parallel and the third one is a mobile transformer with a capacity of 50 MVA. The substation feeds twelve 15 KV feeders, from this five of them (L1, L3, L4, L5, L6, and L7) are from the two winding transformers and six of them (M1, M2, M3, M4, M5, and M6) are from the mobile transformer.

Adama substation II has four incoming lines, two 230 KV from Koka and Huriso, and two 132 KV from Adama substation I and Methara. But the 230 KV is not energized yet. There are two 230/132 KV auto-transformers with a capacity of 125MVA, but it's not energized yet. Additionally, two power transformers (132/15 KV) are there with a capacity of 50 MVA. The substation feeds ten 15 KV feeders from this only two of them (L2 and L3) are energized.

From the 15 KV Adama substation I and II, Adama substation II feeder L2 is selected due to the following reasons:

- High power demand
- High permanent overload power interruption.

The peak load data for Adama substation II, recorded over four months, is presented in Table 3.1.

Table 3.1: September, October, November, and December 2023 peak load data of Adama substation II

Feeder Name	Peak Load							
	September		October		November		December	
	Power (MW)	Current (A)	Power (MW)	Current (A)	Power (MW)	Current (A)	Power (MW)	Current (A)
L2	8.9	350.2	8.99	351.67	9.1	359.69	9.27	363.89

The load data of Adama substation II feeder L2 is given in Table 3.2 below.

Table 3.2: Load data of Adama substation II feeder L2

Bus No.	Peak Load (Kw)	Peak Load (KVar)
1	0	0
2	14	10.5
3	0	0
4	35	28
5	261	235
6	0	0
7	155	110
8	200	155

9	225	175.5
10	189	155
11	13	9.5
12	100	55.5
13	178.5	111
14	15	12.1
15	155	122
16	179	110.75
17	77.7	65
18	19.5	15
19	180	123
20	240	200
21	209.5	160
22	199	167.75
23	217.5	189
24	0	0
25	220	180
26	60	40
27	0	0
28	40	35
29	245	217.5
30	155	120
31	0	0
32	215	170
33	205	193
34	160	120
35	310	290
36	199	155
37	289	213.5
38	14	11.8
39	19	11
40	150	120
41	258	200

42	160	110
43	266	226.7
44	216	181
45	290	178
46	78	55
47	67	40
48	0	0
49	50	39
50	20	13
51	550	492
52	251	200
53	198	109.5
54	0	0
55	180	120
56	110	100
57	34	24
58	538	450
59	410	333
60	65	45
61	14	10.5
62	215	130
63	194	132

3.4. Impedance Calculation of the Overhead Line

The stranded conductor types utilized in the Adama substation II feeder line 2 are AAC-95 (with impedance 0.3085 + j0.2147/km) and AAC-50 (with impedance 0.5787 + j0.4362/km). The conductor's impedance, which is used in the power distribution network, is influenced by the material size, configuration, length, and spacing of the wires. Stranded conductors with a 50 Hz frequency and a length of one kilometer are utilized to determine the inductive reactance. The next step involves calculating the positive sequence impedance using the Equations (3.1) – (3.3) provided below (P. Delivery and S. Member, 1999; P. Grid, 2015).

The conductor impedance measured in ohm can be obtained by using the following equation.

$$Z_a = R_a + j0.06283\ln(\frac{D}{GMR_a})\Omega/km \quad (3.1)$$

$$D = \sqrt[3]{D_{ab}D_{ac}D_{bc}} \quad (3.2)$$

$$GMR_a = k.r \quad (3.3)$$

Where Z_a = conductor impedance in Ω/km

R_a = conductor resistance in Ω/km

$D_{ab,}\ D_{ac,}\ D_{bc}$ = Spacing between conductors a and b, b and c, a and c in meter

GMR_a = Geometric mean radius of conductor a

k = GMR factor

r = Actual conductor radius

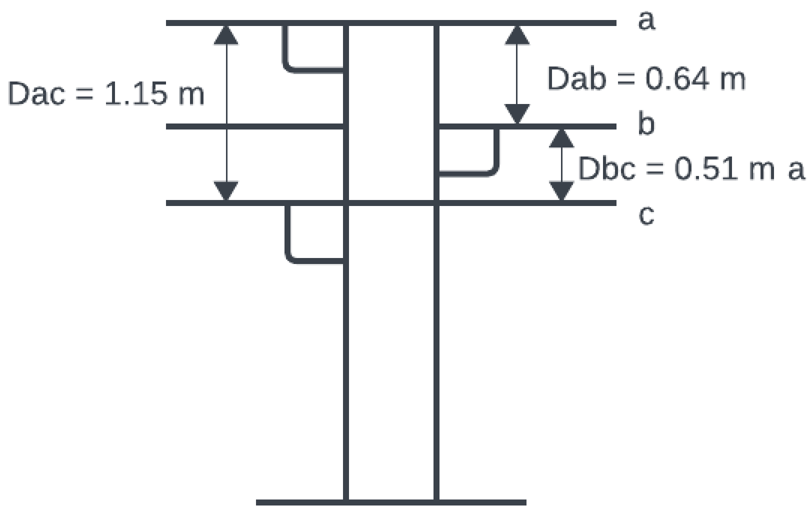

Figure 3.1: Overhead conductor arrangement (by researcher)

Table 3.3: Overhead conductor parameter

Conductor type	Nominal area(mm^2)	Actual area (mm^2)	Strand and wire diameter (mm)	Overall diameter (mm)	Actual diameter (mm)	Resistance (Ω/km)	GMR (mm)
AAC-95	95	93.27	7/3	12.5	10.8975	0.3085	4.129
AAC-50	50	49.48	19/2.5	9	7.9377	0.5785	2.88

Table 3.4: Strand relationship and GMR factor (k) for AAC conductor

Strands	1(solid)	3	7	19	37	61
GMR factor (k)	0.7788	0.6778	0.7256	0.7577	0.7678	0.7722

Using Equations 3.1-3.3, Tables 3.3 and 3.4 we have obtained the following results:

- For the AAC-95 stranded conductor type, the positive sequence impedance is

  $Z_{95} = 0.3085 + j0.3244\ \Omega/km$

- For the AAC-50 stranded conductor type, the positive sequence impedance is

  $Z_{50} = 0.5785 + j0.3470\ \Omega/km$

Therefore, the impedance for the line sections can be calculated by multiplying the length of the line by the impedance of the conductor per kilometer. The impedance value between each bus is given in Table 3.5.

Table 3.5: Adama Substation II 15KV feeder L2 line data

S/N	From bus	To bus	Length (km)	Resistance (ohm)	Reactance (ohm)
1	1	2	0.533	0.3085	0.1850
2	2	3	0.763	0.4413	0.2647
3	3	4	0.340	0.1967	0.1180
4	4	5	0.852	0.4926	0.2955
5	5	6	0.300	0.1736	0.1041
6	6	7	0.350	0.2025	0.1215
7	7	8	0.160	0.0926	0.0555
8	8	9	3.747	2.1678	1.3003
9	9	10	1.969	1.1388	0.6831
10	10	11	1.600	0.9256	0.5552
11	3	12	1.771	1.0248	0.6147
12	12	13	0.490	0.2835	0.1701
13	13	14	0.630	0.3645	0.2186
14	14	15	0.490	0.2835	0.1701
15	15	16	0.690	0.3992	0.2395
16	16	17	0.420	0.243	0.1458

17	13	18	0.410	0.2372	0.1423
18	18	19	0.130	0.0752	0.0451
19	19	20	0.370	0.214	0.1284
20	20	21	0.420	0.243	0.1458
21	21	22	0.340	0.1967	0.1180
22	6	23	0.959	0.5545	0.3326
23	23	24	0.350	0.2025	0.1215
24	24	25	0.460	0.2661	0.1596
25	25	26	0.490	0.2835	0.1701
26	26	27	2.119	1.2256	0.7351
27	27	28	1.596	0.9231	0.5537
28	28	29	0.480	0.2777	0.1666
29	29	30	2.099	1.214	0.7282
30	30	31	0.850	0.4917	0.2949
31	31	32	1.071	0.6198	0.3718
32	32	33	0.471	0.2727	0.1636
33	26	34	0.220	0.1273	0.0764
34	34	35	0.420	0.243	0.1458
35	35	36	0.390	0.2256	0.1353
36	26	37	0.713	0.4124	0.2474
37	37	38	0.130	0.0752	0.0451
38	27	39	0.690	0.3992	0.2395
39	39	40	0.220	0.1273	0.0764
40	28	41	3.707	2.1446	1.2864
41	41	42	1.979	1.1446	0.6866
42	42	43	2.039	1.1793	0.7074
43	43	44	2.009	1.162	0.6970
44	44	45	0.350	0.2025	0.1215
45	31	46	0.160	0.0926	0.0555
46	46	47	0.310	0.1793	0.1075
47	24	48	0.330	0.1909	0.1145
48	48	49	0.045	0.026	0.0156
49	49	50	0.160	0.0926	0.0555

50	50	51	1.800	1.0411	0.6245
51	48	52	0.910	0.5264	0.3157
52	52	53	0.120	0.0694	0.0416
53	53	54	0.140	0.081	0.0486
54	54	55	0.200	0.1157	0.0694
55	55	56	0.440	0.2545	0.1527
56	56	57	0.100	0.0578	0.0347
57	54	58	0.210	0.1215	0.0729
58	58	59	1.001	0.5793	0.3475
59	8	60	1.759	1.0174	0.6103
60	60	61	0.250	0.1446	0.0867
61	61	62	0.600	0.3471	0.2082
62	62	63	0.900	0.5206	0.3123

3.5. Analysis of Solar Radiation Data of Adama City

Before installing a solar panel in a particular location, it's recommended to assess the suitability of implementing solar power-based DG in that area. Thus, in the design process of a PV system, analyzing solar radiation availability is crucial for determining input variables. Solar radiation data can be obtained in various formats from different sources, such as meteorological agencies and NASA. Photovoltaic cells should generate energy when exposed to sunlight and solar irradiation. PV cells must be able to produce energy during the hours of sunlight and solar irradiation. Therefore, daylight hours were taken into account during design, and according to (Gana & Akpootu, 2013), solar radiation has to be between 4-6 KWh/m^2/day. The solar radiation measured data of 7 years for Adama city collected from Ethiopian National Metrology and NASA, is shown in Tables 3.6 and 3.7.

Table 3.6: Solar radiation data of Adama city (Mesgana Tulu, 2023)

Month	Jan	Feb	Mar	Apr	May	Jun	Jul	Aug	Sep	Oct	Nov	Dec
Solar radiation (Kwh/m^2/ day)	6.02	6.51	6.74	6.4	6.47	6.23	5.61	5.72	5.92	6.21	6.14	5.96

Table 3.7: Solar radiation data of Adama city [NASA]

RETScreen - Climate database

Map | Search | Data

Country		Ethiopia	
Province/State		n/a	
Climate data location	See map	Nazrēt	
Latitude	°N	8.6	
Longitude	°E	39.3	**Source**
Climate zone	3A	Warm - Humid	NASA
Elevation	m	1,869	NASA
Heating design temperature	°C	11.6	NASA
Cooling design temperature	°C	26.4	NASA
Earth temperature amplitude	°C	15.5	NASA

Month	Air temperature	Relative humidity	Precipitation	Daily solar radiation - horizontal	Atmospheric pressure	Wind speed	Earth temperature	Heating degree-days 18 °C	Cooling degree-days 10 °C
	°C	%	mm	kWh/m²/d	kPa	m/s	°C	°C-d	°C-d
January	18.5	44.2%	22.02	6.08	81.5	3.4	22.7	0	263
February	20.1	38.8%	14.50	6.57	81.4	3.1	25.0	0	281
March	21.5	40.3%	61.04	6.52	81.4	3.0	26.7	0	358
April	21.5	49.6%	58.11	6.31	81.3	3.1	26.3	0	344
May	21.3	53.9%	60.25	6.36	81.4	2.9	25.4	0	349
June	19.5	66.2%	109.74	5.77	81.4	2.9	21.8	0	284
July	18.2	70.2%	203.93	5.23	81.4	2.5	19.7	0	255
August	18.1	71.2%	167.25	5.36	81.4	2.3	19.3	0	251
September	18.6	66.1%	84.86	5.84	81.4	2.3	20.3	0	257
October	18.8	54.3%	52.22	6.31	81.5	2.8	21.3	0	271
November	18.3	46.5%	14.96	6.27	81.5	3.2	21.5	0	250
December	17.9	47.9%	11.30	6.08	81.5	3.4	21.5	5	243
Annual	**19.3**	**54.2%**	**860.17**	**6.05**	**81.4**	**2.9**	**22.6**	**5**	**3,405**
Source	NASA	NASA	NASA	NASA	NASA	NASA	NASA	NASA	NASA
Measured at					m	10	0		

As shown in the above tables the solar radiation of Adama city is enough to install solar-based DG in the selected area.

3.6. Load Flow Analysis for Radial Distribution System

Load flow analysis plays a crucial role in regulating power systems as it allows us to compute the voltages at each bus and the currents at every branch. Numerous analyses would be impossible without the load flow analyses since it provide essential data about the power system. Several power systems applications, like network reconfiguration, distributed generation and FACTS device placements, power quality enhancements, service restorations, economic dispatch, power systems optimization, and others, use load flow analysis, whether directly or indirectly(Kidane Tsehay Asrat, 2023). Various load flow techniques have been utilized to develop power flow analysis in both distribution and transmission systems. Gauss-Seidel, fast-decoupled and Newton-Raphson load flow techniques are commonly employed in power transmission systems. However, it has been consistently demonstrated by different researchers, that these methods may prove ineffective when employed to analyze distribution systems because of the distinct characteristics of such networks. These include radial structure, low reactance-resistance (X/R) ratio, unbalanced loads, and un-transposed lines, as well as single-phase and two-phase laterals (Kefeni Getahun Shanko, 2023).

The two primary methods often employed in analyzing load flow in distribution systems are the BFS and the DLF techniques (Kumar Pujari, 2020). The main features of these load flows are simplicity, low memory requirements, and high efficiency in producing accurate solutions throughout the entire process. However, the DLF method achieves faster computational time compared to the BFS approach (Kawambwa et al., 2021). This paper employs direct load flow analysis, which is favored for its faster computational time and simplicity, and it is suitable for distribution systems.

3.6.1. Direct Load Flow Method

The initial proposal by (Teng, 2003) for the direct load flow technique relies on computing two matrices: the bus injection to branch current (BIBC) and the branch current to bus voltage (BCBV). Subsequently, the DLF matrix is derived by multiplying BIBC and BCBV. Notably, the DLF method yields faster computational time in comparison to the BFS technique.

Relationship Matrix Development

A more practical model in distribution systems is the equivalent current injection-based model. The complex load power S_i for bus i, is given by:

$$S_i = (P_i + jQ_i) \qquad i = 1,2,3 \dots . N \tag{3.4}$$

The equivalent i^{th} bus current injection at the kth iteration can be expressed as:

$$I_i^k = I_i^r(V_i^k) + jI_i^i(V_i^k) = \left(\frac{P_i + jQ_i}{V_i^k}\right)^* \tag{3.5}$$

Where I_i^k and V_i^k are the equivalent current injections and bus voltages of bus i, at the k^{th} iteration respectively I_i^i and I_i^r are the imaginary and real parts of the equivalent current injection of bus i, at the k^{th} iteration respectively P_i and Q_i are the real and imaginary parts of the load power at bus i, respectively. The depicted simple distribution system in Figure 3.2 serves as an example to create the BIBC and BCBV matrix. Using Equation (3.5), power injections are converted into equivalent current injections. The relationship between bus branch currents and current injections is then determined by applying Kirchhoff's Current Law (KCL) to the distribution system. The branch currents can be expressed in terms of equivalent current injections. For instance, the branch currents $\mathrm{IB}_1, \mathrm{IB}_2, \mathrm{IB}_3, \mathrm{IB}_4$ and IB_5 can be formulated based on the equivalent current injections as the following equations.

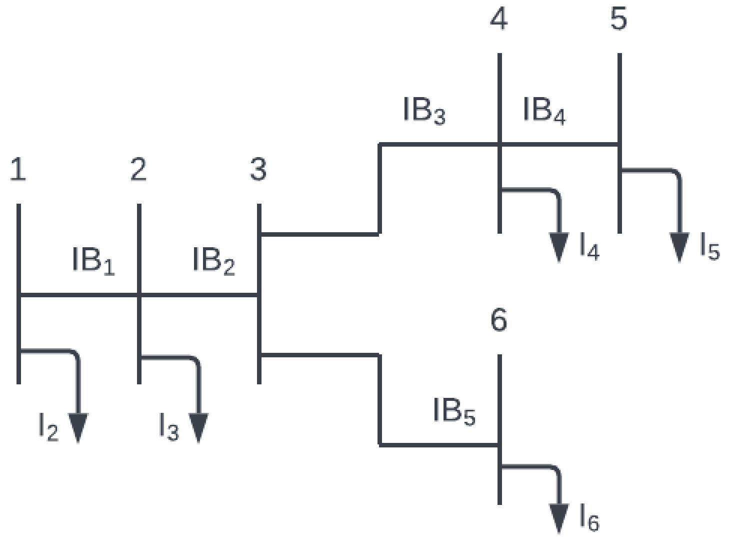

Figure 3.2: Sample distribution system (Abu-Moti & EI-Hawary, 2011)

$$\begin{aligned}
&\mathrm{IB}_1 = \mathrm{I}_2 + \mathrm{I}_3 + \mathrm{I}_4 + \mathrm{I}_5 + \mathrm{I}_6 \\
&\mathrm{IB}_2 = \mathrm{I}_3 + \mathrm{I}_4 + \mathrm{I}_5 + \mathrm{I}_6 \\
&\mathrm{IB}_3 = \mathrm{I}_4 + \mathrm{I}_5 \\
&\mathrm{IB}_4 = \mathrm{I}_5 \\
&\mathrm{IB}_5 = \mathrm{I}_6
\end{aligned} \tag{3.6}$$

And, know if we rewrite Equation (3.6) in matrix form it becomes: -

$$\begin{bmatrix} \mathrm{IB}_1 \\ \mathrm{IB}_2 \\ \mathrm{IB}_3 \\ \mathrm{IB}_4 \\ \mathrm{IB}_5 \end{bmatrix} = \begin{bmatrix} 1 & 1 & 1 & 1 & 1 \\ 0 & 1 & 1 & 1 & 1 \\ 0 & 0 & 1 & 1 & 0 \\ 0 & 0 & 0 & 1 & 0 \\ 0 & 0 & 0 & 0 & 1 \end{bmatrix} \begin{bmatrix} \mathrm{I}_2 \\ \mathrm{I}_3 \\ \mathrm{I}_4 \\ \mathrm{I}_5 \\ \mathrm{I}_6 \end{bmatrix} \tag{3.7}$$

Equation (3.7) can be re-expressed as follows:

$$[\mathrm{IB}] = [\mathrm{BIBC}][\mathrm{I}] \tag{3.8}$$

Where: BIBC is a bus injection to branch current matrix, IB_i is a branch current, and I_i are current injections at bus *i*.

The relationship between bus voltage and branch current which is illustrated in Figure 3.2 can be expressed as the following equations: -

$$\begin{aligned}
V_2 &= V_1 - IB_1 Z_{12} \\
V_3 &= V_1 - IB_1 Z_{12} - IB_2 Z_{23} \\
V_4 &= V_1 - IB_1 Z_{12} - IB_2 Z_{23} - IB_3 Z_{34} \\
V_5 &= V_1 - IB_1 Z_{12} - IB_2 Z_{23} - IB_3 Z_{34} - IB_4 Z_{45} \\
V_6 &= V_1 - IB_1 Z_{12} - IB_2 Z_{23} - IB_5 Z_{56}
\end{aligned} \tag{3.9}$$

Equation (3.9) shows that the bus voltage depends on the values of the line parameters, substation voltage, and branch currents. Therefore, by rearranging Equation (3.9) above, then the relationship between bus voltages and branch currents can be expressed as: -

$$\begin{bmatrix} V_1 \\ V_1 \\ V_1 \\ V_1 \\ V_1 \end{bmatrix} - \begin{bmatrix} V_2 \\ V_3 \\ V_4 \\ V_5 \\ V_6 \end{bmatrix} = \begin{bmatrix} Z_{12} & 0 & 0 & 0 & 0 \\ Z_{12} & Z_{23} & 0 & 0 & 0 \\ Z_{12} & Z_{23} & Z_{34} & 0 & 0 \\ Z_{12} & Z_{23} & Z_{34} & Z_{45} & 0 \\ Z_{12} & Z_{23} & 0 & 0 & Z_{36} \end{bmatrix} \begin{bmatrix} IB_1 \\ IB_2 \\ IB_3 \\ IB_4 \\ IB_5 \end{bmatrix} \tag{3.10}$$

Again Equation (3.10) can be rewritten in general form as: -

$$[\Delta V] = [BCBV][IB] \tag{3.11}$$

Where BCBV is the branch current to bus voltage matrix, and V_i are the *i* bus voltages.

To create the BIBC and BCBV matrix for a universal network, the following steps can be utilized.

Algorithm for BIBC matrix formation

By observing Equation (3.7) a construction algorithm for the BIBC matrix can be created as follows:

Step 1. In a distribution system with p branch sections and q buses, the dimension of the BIBC matrix is p *x* (q-1).

Step 2. If a line section IB_k is situated between bus *i* and bus *j*, copy the column of the *i*th bus of the BIBC matrix to the column of the *j*th bus and then put +1 to the position of the *k*th row and the *j*th bus column.

Step 3. Continue performing step 2 until all line sections are encompassed in the BIBC matrix.

Algorithm for BCBV matrix formation

By observing equation (3.10) a construction algorithm for the BCBV matrix can be developed as follows:

Step 1. In a distribution system with p branch sections and q buses, the dimension of the BIBC matrix is (q-1) *x* p.

Step 2. If a line section IB_k is situated between bus *i* and bus j, copy the row of the i^{th} bus of the BCBV matrix to the row of the j^{th} bus and then put the line impedance (Z_{ij}) to the position of the k^{th} row and the j^{th} bus column.

Step 3. Continue performing Step 2 until all line sections are encompassed in the BCBV matrix.

By combining Equations (3.8) and (3.11), we get the following equation that relates bus current injections to bus voltages:

$$[\Delta V] = [BCBV][BIBC][I] \tag{3.12}$$

$$[\Delta V] = [DLF][I] \tag{3.13}$$

Where,

$$[DLF] = [BCBV][BIBC] \tag{3.14}$$

3.6.2. Algorithm of DLF for Distribution Networks

The algorithmic procedures for determining distribution network load flow solutions are given in the following steps.

Step 1: Read the line and bus data of distribution networks.

Step 2: Compute the injection matrix for each node using Equation (3.5).

Step 3: Formulate the BIBC matrix.

Step 4: Using Equation (3.8) compute the branch current from the BIBC and injection current matrix.

Step 5: Formulate the BCBV matrix.

Step 6: Using Equation (3.14) compute the DLF matrix.

Step 7: Define k = 0 and start iteration k = k + 1.

Step 8: Update voltages through the following equation:

$$I_i^k = I_i^r(V_i^k) + jI_i^i(V_i^k) = \left(\frac{P_i + jQ_i}{V_i^k}\right)^* \quad (3.15)$$

$$\Delta V^{k+1} = [\mathrm{DLF}][I_i^k] \quad (3.16)$$

$$V^{k+1} = V_1 - \Delta V^{k+1} \quad (3.17)$$

Step 9: Check stopping criteria if max $|(V^{k+1} - V^k)| >$ tolerance go to step 8.

Step 10: Determine the losses and branch currents from the final bus voltages.

Step 11: Show the branch losses and bus voltage magnitudes.

Step 12: Stop

3.7. Incorporating DG and DSTATCOM into Load Flow

The Distributed Generation (DG) units, modeled as PQ nodes, can be handled as negative PQ loads in load flow without any issues. Let's consider a radial distribution network with a single source and NL branches. A DG source will be connected to the network at bus i. While it is common knowledge that DG supplies active power (PG^{DG}) to the systems, supplying or consumption of reactive power (QG^{DG}) is contingent upon the DG source. But in this thesis DG type I is used which supplies only active power (PG^{DG}). And, DSTATCOM is connected to the network at bus j and may absorb or supply reactive power ($QG^{DSTATCOM}$) to the system. The active and reactive power injection at buses i and j results in the flow of an active current and a reactive current through the system, altering the active and reactive components of the bus voltage and the branch current between all buses. Before integrating DG and DSTATCOM, the apparent power is given by: -

$$S_i^{without\_DG\_DS} = PD_i + jQD_i \qquad i = 1,2,3, \dots NB \quad (3.18)$$

And, the current injection at bus i is given by: -

$$I_i^{without\_DG\_DS} = \left(\frac{S_i^{without\_DG\_DS}}{V_i}\right)^* \qquad i = 2,3, \dots NB \quad (3.19)$$

After placement of DG and DSTATCOM at bus i and j respectively, the active and reactive power at bus i and j is modified as: -

$$P_i^{with\_DG} = PD_i + PG^{DG} \quad (3.20)$$

$$Q_j^{with\_DS} = QD_j \pm QG^{DSTATCOM} \quad (3.21)$$

The apparent power is computed using Equation (3.22) after integrating DG and DSTATCOM.

$$S_i^{with\_DG\_DS} = P_i^{with\_DG} + Q_i^{with\_DS} \qquad i = 2,3, \dots NB \qquad (3.22)$$

The current injection at bus i is given by: -

$$I_i^{with\_DG\_DS} = \left(\frac{S_i^{with\_DG\_DS}}{V_i}\right)^* \qquad i = 2,3, \dots NB \qquad (3.23)$$

3.8. Problem Formulation

The goal is to identify the appropriate size and location of DG and DSTATCOM while taking into account the objective function and constraints, ensuring that all operating conditions are not violated. The objective function and constraints are included in the algorithm's problem formulation.

A. Objective Function

The objective function of the research involves minimizing active and reactive power loss and enhancing the voltage profile. The objective function is then utilized to determine the size and location of DG and DSTATCOM, considering the weighting coefficients for each one. In the following subsections, these objective functions were mathematically formulated.

Active power loss

The active power losses within the distribution network can be computed in the following manner:

$$f_1 = P_{loss} = \sum_{i=1}^{nb} R_i i_i^2 \qquad (3.24)$$

Where

P_{loss}: is active power loss,

f_1: is an objective function representing active power loss,

R_i: is the line resistance of branch i,

i_i: is the branch current of branch i,

n_b: is the number of system branches.

Reactive power loss

The active power losses within the distribution network can be computed as follows:

$$f_2 = Q_{loss} = \sum_{i=1}^{nb} X_i i_i^2 \tag{3.25}$$

Where

Q_{loss}: is reactive power loss,

f_2: is an objective function representing reactive power loss,

X_i: is the line reactance of branch i,

Voltage Profile Enhancement

The objective function for enhancing the voltage profile is as expressed follows.

$$f_3 = \sum_{i=1}^{nbus} (V_{norm} - V_i)^2 \tag{3.26}$$

Where,

f_3: Represents the objective function for the voltage profile enhancement,

V_{norm}: Represents the system's nominal voltage, which is set to 1 p.u,

V_i: Represents the voltage of the i^{th} bus,

nbus: Number of system buses.

The general objective function is mathematically expressed as:

$$F = w_1 * f_1 + w_2 * f_2 + w_3 * f_3 \tag{3.27}$$

The weighting coefficients $w_1,\ w_2\ and\ w_3$ are determined based on the relative significance of the three objectives, ensuring that their sum equals 1: $\sum_{n=1}^{3} w_n = 1$. In this work 0.5, 0.1, and 0.4 are used as the values of $w_1,\ w_2\ and\ w_3$ respectively.

B. System Constraints

The optimal sizing and placement of DG and DSTATCOM in the distribution network are subject to the following constraints:

DG and DSTATCOM Size Constraints

To achieve the best outcome, the size of both DG and DSTATCOM must be appropriately matched with the load value, avoiding being either too small or excessively large. The system has defined limits for the lowest and highest amounts of active power that the DG can supply and for the reactive power that the DSTATCOM can inject.

$$PG_{min}^{DG} \le PG^{DG} \le PG_{max}^{DG} \tag{3.28}$$

$$QG_{min}^{DSTATCOM} \leq QG^{DSTATCOM} \leq QG_{max}^{DSTATCOM} \tag{3.29}$$

Where PG_{min}^{DG} *and* PG_{max}^{DG} are the minimum and maximum size active power generated by DG respectively, $QG_{min}^{DSTATCOM}$ *and* $QG_{max}^{DSTATCOM}$ are the minimum and maximum size of reactive power generated by DSTATCOM and then injected into the system.

DG and DSTATCOM location Constraint

DG and DSTATCOM location constraint is the number of bus limits for where we put them on is defined as

$$2 \leq DG_{location} \leq N_b \tag{3.30}$$

$$2 \leq DSTATCOM_{location} \leq N_b \tag{3.31}$$

Where N_b is the total number of buses and $N_b = 63$.

Bus voltage constraints

This encompasses the minimum and maximum voltage magnitude limits, V_i^{min} *and* V_i^{max} at bus i. The voltage at every bus must kept in the permissible range of bus voltages. This can be expressed as follows:

$$V_i^{min} \leq V_i \leq V_i^{max} \tag{3.32}$$

Where $V_i^{min} = 0.95$ is the minimum *and* $V_i^{max} = 1,$ is the maximum bus voltages respectively.

3.9. Optimal Sizing and Positioning of DG and DSTATCOM

The objective of this section is to identify the optimal size and place of DG and DSTATCOM through the utilization of Particle Swarm Optimization (PSO).

3.9.1. Particle Swarm Optimization (PSO)

PSO, is an ingenious optimization technique that draws inspiration from the movement and intelligence exhibited by swarms in nature. It effectively harnesses the power of social interactions to solve complex problems. James Kennedy (a social psychologist) and Russell Eberhart (an electrical engineer) co-developed it in 1995(Witoon Prommee & Weerakorn Ongsakul, 2008). The particle swarm represents a social structure or system model inspired by basic creatures that form groups with specific objectives, such as food searching. It plays a crucial role in maximizing the population's potential within the group that engages in the same activities. This relative behavior is observed in various groups of creatures, like a swarm of bees, a school of fish, or a flock of birds.

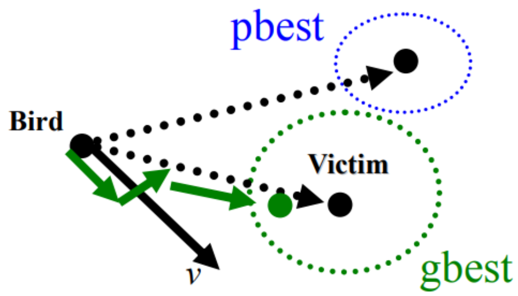

Figure 3.3: Birds' food searching with PSO (Witoon Prommee & Weerakorn Ongsakul, 2008)

In Figure 3.3, a bird flock hunter is presented as a bird susceptible to a particle. During victim searching, all bird groups will navigate together in a unified direction. The bird leader is the one closest to the food source with the shortest distance, considered to have the best fitness, and the remaining birds trail behind, following the leader. The fitness value consideration will involve the usage of the particle swarm model, with the particles representing fitness value solutions. Furthermore, in the context of food searching in birds, an essential property involves the utilization of each particle's velocity to determine the direction of particle movement. Consequently, all particles within the flock must adjust their direction based on the best fitness of particle direction. This iterative process ultimately aids in establishing the most suitable direction.

3.9.1.1. Basics to Particle Swarm Optimization

A particle swarm is made up of i particles in the basic particle swarm optimization technique, and each particle's position represents a possible solution and has a fitness value in D-dimensional space. Fitness is assessed and needs to be optimized. The particles change their state according to three main principles (Pandey & Singh Bhadoriya, 2014):

- To maintain its inertia
- To adjust the situation to its most optimistic state
- To adjust the situation in accordance with the swarm's most optimistic viewpoint.

The position of every particle is guided by a predetermined velocity, which is updated during each iteration. Particles eventually gravitate toward the optima due to their ideal position and the best solution the group has ever experienced. A particle's velocity is updated based on: its prior velocity, its best position found so far, and the best position discovered by the entire swarm (Abayneh & Fekadu Shewarega, 2022). Every particle maintains track of its search space coordinates, associated with the particle's current best solution (fitness) and named personal best, or (pbest). The best value that any particle in the neighborhood of that particle has obtained thus far is another best value that the PSO continuously tracks. The value is known as global best (gbest) (Pandey & Singh Bhadoriya, 2014). The PSO modifies the velocity and, thus, the position of every particle with each iteration. The random value weighted acceleration is used to accelerate the position of the particle toward pbest and gbest. The prior velocity and the difference between the previous position and pbest and gbest can be used to compute the prevailing velocity. The following equation can be used to update the position and velocity of each particle(Gad, 2022):

$$V_{id}^{k+1} = wV_{id}^{k} + c_1 r(P_{best\,id} - X_{id}^{k}) + c_2 r(G_{best\,id} - X_{id}^{k}) \quad (3.33)$$

$$X_{id}^{k+1} = X_{id}^{k} + V_{id}^{k+1} \quad (3.34)$$

Where: i = 1,2,3…n (number of particles) and d=1,2,3…D (dimensions)

V_{id}^{k+1} − Modified velocity of particle '*i*'

V_{id}^{k} − Current velocity of particle '*i*'

w − Inertia weight

c_1, c_2 − Acceleration coefficients

$P_{best\,id}$ − Personal best value of the particles

$G_{best\,id}$ − Global best value of the group

X_{id}^{k} − Current position of the particle

X_{id}^{k+1} − Modified position of the particle

r - A randomly generated value added to the model to introduce stochastic nature, within the interval [0 1].

k – Number of iterations

The weight function is calculated as:

$$w = w_{max} - \frac{(w_{max} - w_{\min})}{max_{iter}} * k \tag{3.35}$$

Where: $\mathrm{w_{max}}$ and $\mathrm{w_{min}}$ are the minimum and maximum weights respectively

max_{iter} – Maximum iteration

3.9.1.2. PSO Parameters

Several parameters in the PSO method can impact its effectiveness for a particular optimization task. The performance of the PSO technique is heavily influenced by certain parameter values and selections, while less or no effect is produced by others. The fundamental PSO parameters are (Pandey & Singh Bhadoriya, 2014; Abayneh & Fekadu Shewarega, 2022):

Swarm size: The number of particles (n) in the swarm is the population size, often known as the swarm size. By employing more particles, fewer iterations will be required to achieve a satisfying optimization outcome. However, using more particles will increase the computational complexity per iteration and increase the time required.

Particle velocity: The current velocity $\mathrm{V_{id}^{K}}$ is limited within the intervals $\mathrm{V_{id}^{min}} \leq \mathrm{V_{id}^{K}} \leq \mathrm{V_{id}^{max}}$. The parameters $\mathrm{V_{id}^{max}}$ define the resolution or fitness, guiding the search for regions between the current and target positions. When $\mathrm{V_{id}^{max}}$ is extremely high, particles may overshoot the best solutions. This occurs because particles take larger steps, potentially missing the optimal solution. Likewise, if $\mathrm{V_{id}^{min}}$ is too little, particles require more time to reach the optimal solutions. When updating the particle’s velocity, the velocity components are crucial. A particle's velocity typically consists of three terms: the inertia component, the social component, and the cognitive component.

- The term $\mathrm{V_{id}^{K}}$ is known as the inertia component. It helps maintain the particle's momentum, preventing abrupt changes in direction and encouraging the particle to continue moving in its current trajectory. It reflects the movement's recent history, helping to prevent sudden changes in the particle's direction and allowing the particle to continue in its current path.
- The term $\mathrm{c_1 r(P_{best\,id} - X_{id}^{k})}$ is referred to as the cognitive component. It evaluates the particle's performance based on previous achievements, serving as their memory of the best position. This component guides the particles towards positions that have been most satisfactory for them in the past.

- The term $c_2r(G_{best\,id} - X^k_{id})$ for gbest PSO is known as the social component. This term assesses the particle's performance concerning a group of particles, directing each particle toward the best position discovered by the agent's neighborhood.

Random numbers: It is a uniform random value, ranging from 0 to 1, contributing to creating the stochastic nature of PSO.

Accelerating coefficients: In particle swarm optimization (PSO), the acceleration coefficients, c1, and c2, govern the influence of the social and cognitive components in updating a particle's velocity. These coefficients, along with randomly generated numbers r1 and r2, determine the stochastic nature of the velocity update. c1 represents a particle's self-confidence, while c2 represents the confidence a particle has in its neighbors. The characteristics of c1 and c2 are as follows: (Abayneh & Fekadu Shewarega, 2022; Gad, 2022):-

- The situation where c1 and c2 are both zero leads to agents maintaining their current speeds until the search space boundary is reached.
- For c1 greater than c2, each agent is substantially impacted by its personal best position, potentially leading to local traps.
- When c1 is less than c2, all swarm agents are significantly influenced by the global best position, causing premature convergence towards the optimum, possibly leaving parts of the search space unexplored.
- If c1 equals c2, all agents are pulled to the average of Pbest and Gbest.

Properly setting up c1 and c2 is essential for achieving the best results. Making incorrect assumptions about c1 and c2 can lead to repetitive behavior. Multiple studies suggest that setting both acceleration constants to two (2) is ideal for optimal performance (Abayneh & Fekadu Shewarega, 2022; Gad, 2022).

Inertia weight: This parameter regulates how the current velocity relates to the prior velocity. Usually, the inertia weight (w) is modified based on the Equation 3.35 above. Suitable values for w_{min} and w_{max} are 0.4 and 0.9, respectively.

Termination criterion: Optimization algorithms typically employ a stopping criterion to determine when to terminate the search process. This criterion may involve reaching a predefined maximum number of iterations or achieving the required degree of accuracy in the solution.

3.9.1.3. Merits and Demerits of PSO

Merits of PSO: -

- It applies to both scientific research and engineering.
- It is easy to implement
- Its exclusion of overlapping and mutation calculations.
- Minimal algorithm parameters.
- Highly efficient global search algorithm.
- Easily parallelized for concurrent processing.

Demerits of PSO: -

- The method exhibits partial optimism, resulting in less precise control over its velocity and direction.
- The method may encounter challenges when dealing with non-coordinate system problems, such as determining solutions for energy fields and establishing movement rules for particles within these energy fields.

The PSO flow chart is shown in Figure: 3.4 below

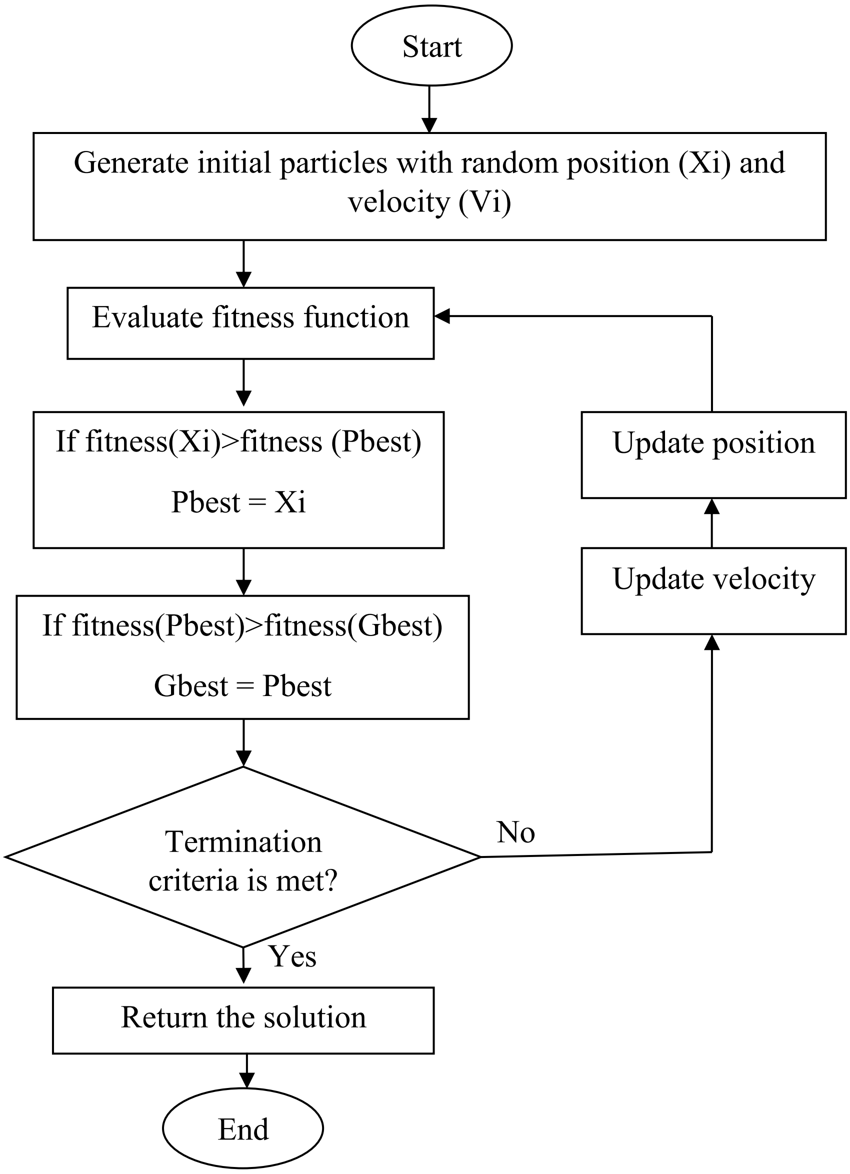

Figure 3.4: PSO flow chart (Pandey & Singh Bhadoriya, 2014)

3.10. The PSO Algorithm with Optimal Positioning and Sizing of DG and DSTATCOM

The following steps can be accomplished objectively using the PSO technique to address the DG and DSTATCOM placement and size issues.

Step 1: Read the line data and bus data which are saved in MATLAB as m_file.

Step 2: Initialize the Swarm parameters:

- Establish the limits of the DG and DSTATOM location and size as well as the velocity Vmax and Vmin.

- Indicate the values of the acceleration coefficients c1 and c2 as well as the inertial weight w.
- Assign the initial velocity and position ($X_i = [X_1, X_2,...,Xn]$, and $V_i = [V_1, V_2,...,Vn]$).
- Generate a random initial population of N particles with a D-dimensional search space.

Step 3: Run the load flow with DG and DSTATCOM to determine the voltage at each bus and power loss in the distribution system for the respective DG and DSTATCOM sizes and positions to assess each particle's fitness. Power loss reduction and voltage deviation are both taken into account by the fitness function.

Step 4: Based on the fitness and dominance of each particle, update the Pbest for that particle.

Step 5: Update Gbest by figuring out which particles have non-dominated solutions.

Step 6: Look for convergence requirements, such as the maximum number of iterations or an acceptable degree of convergence. Repeat Steps 3 to 7 if the convergence conditions are not satisfied, if the convergence condition is satisfied go to step 8.

Step 7: Update the particle's velocity and position using Equations (3.33) and (3.34) respectively and go to step 3.

Step 8: Display the result: power losses, voltage profile, DG and DSTATCOM size and location.

Below is a flowchart outlining the implementation of DG and DSTATCOM sizing and siting using PSO:

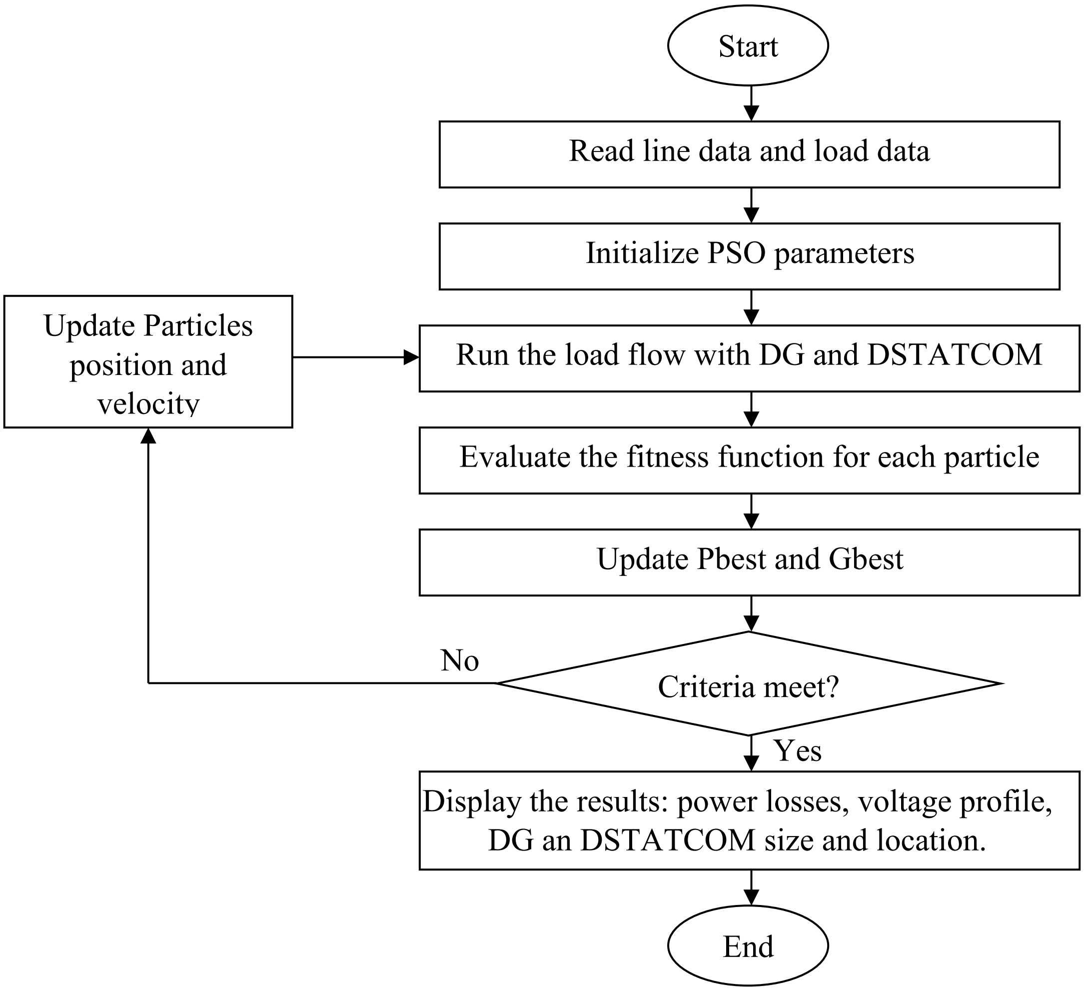

Figure 3.5: PSO flow chart for the implementation of placement and sizing of DG and DSTATCOM

CHAPTER FOUR

4. RESULTS AND DISCUSSIONS

4.1. Introduction

This chapter focuses on the results and their depth discussions based on the data collected in the preceding chapter and facilitated by the previously developed algorithm. The PSO algorithm elaborated in the previous section has been implemented and programmed using MATLAB 2022b software. The main program developed based on the implementation procedures of the suggested algorithm is provided in the Appendix. The results of this study are analyzed and presented in four different cases, as discussed in the next section.

4.2. System Performance under Different Cases

Case I: System Performance of Base Case (Without DG and DSTATOM)

In this case, the base case load flow simulation is executed to investigate the present status of the distribution system. The analysis of load flow was carried out utilizing a direct load flow method, programmed in MATLAB, whose main program is available in the Appendix. By utilizing the line data and bus data from the distribution system within the case study of Adama Substation II, line 2, the MATLAB direct load flow was simulated.

Figures 4.1, 4.2, and 4.3 show the base case voltage profiles, active power losses, and reactive power losses of the network, respectively. The minimum voltage is at bus 45 having a value of 0.75141, which is below the lower threshold limit (0.95 pp.). Bus number one and two are the only buses, their voltage is between the allowable range i.e. 0.95 to 1.05 p.u. The total active and reactive power loss of the system under base case is 1862.9 KW and 1204.5 kVar respectively.

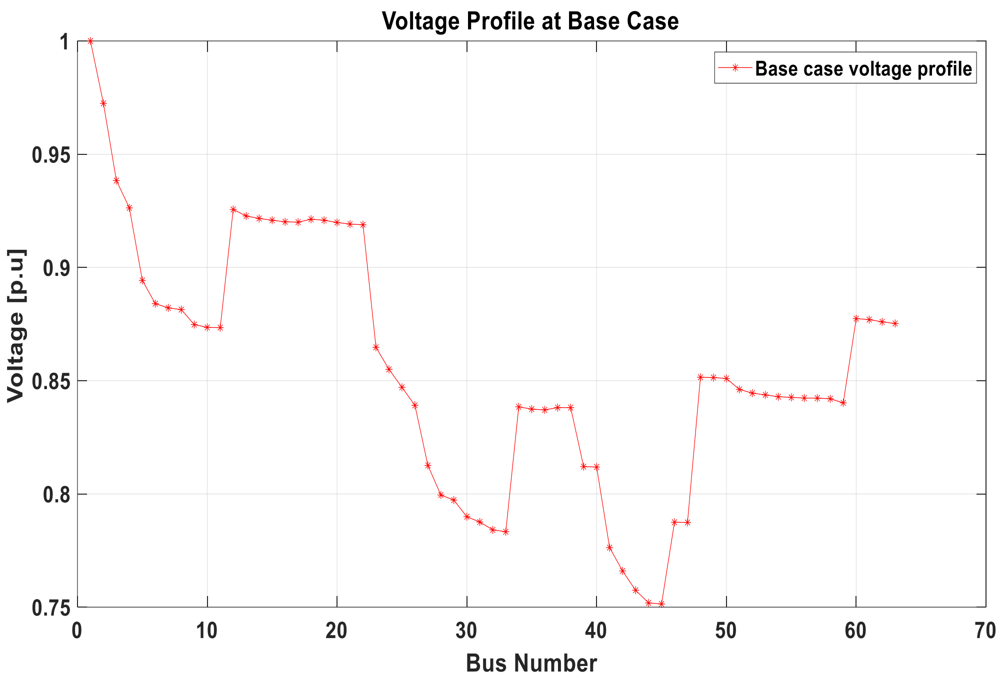

Figure 4.1: Voltage profile (p.u) at base case

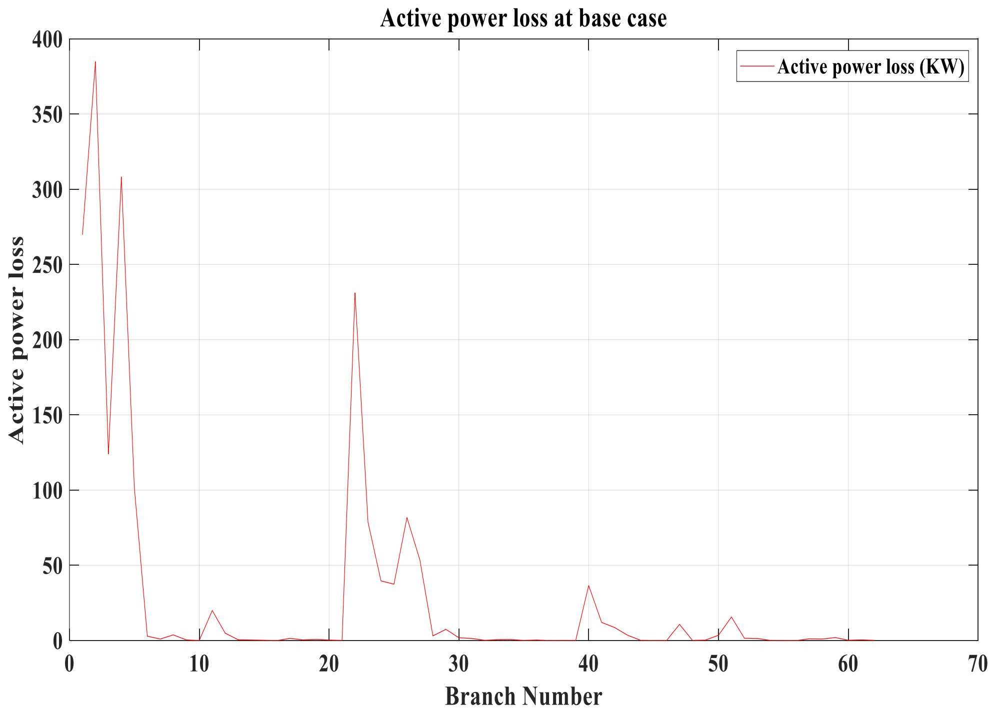

Figure 4.2: Active power loss (KW) at base case

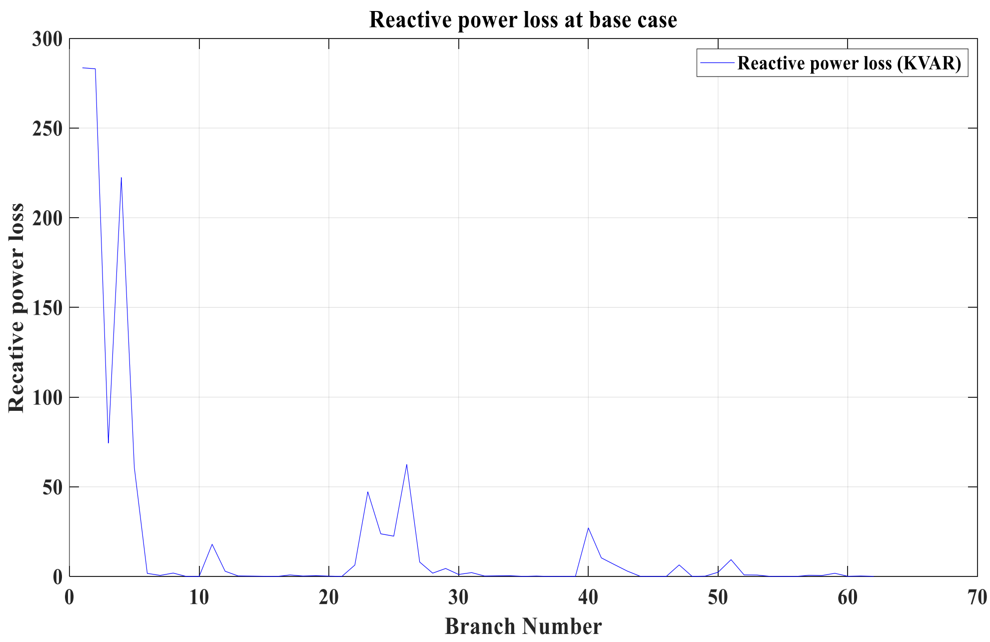

Figure 4.3: Reactive power loss (KVAR) at base case

Case II: System Performance with one DG

In this case, a load flow with a single DG is executed to evaluate the performance of the distribution system. To find the best placement and capacity of DG units, a PSO algorithm is used. The goal is to reduce the real, reactive power losses, and the voltage deviation, using Equation 3.27 as the objective function.

Bus 27 has been identified as the best place for the DG allocation, and its optimal size is 4 MW. The voltage profile of the network after a single DG is allocated at bus no. 27 is presented in Figure 4.4 and the obtained active and reactive power losses are presented in Figures 4.5 and 4.6 respectively. In this case, the minimum voltage is at bus 45 with a value of 0.8745, which is lower than the threshold voltage limit (i.e. 0.95 p.u). In this case, only four buses have voltages within the acceptable range, specifically ranging from 0.95 to 1.05 p.u. The total real and reactive power losses of the network after a single DG is allocated are reduced to 870.0948 KW and 576.5648 kVar respectively.

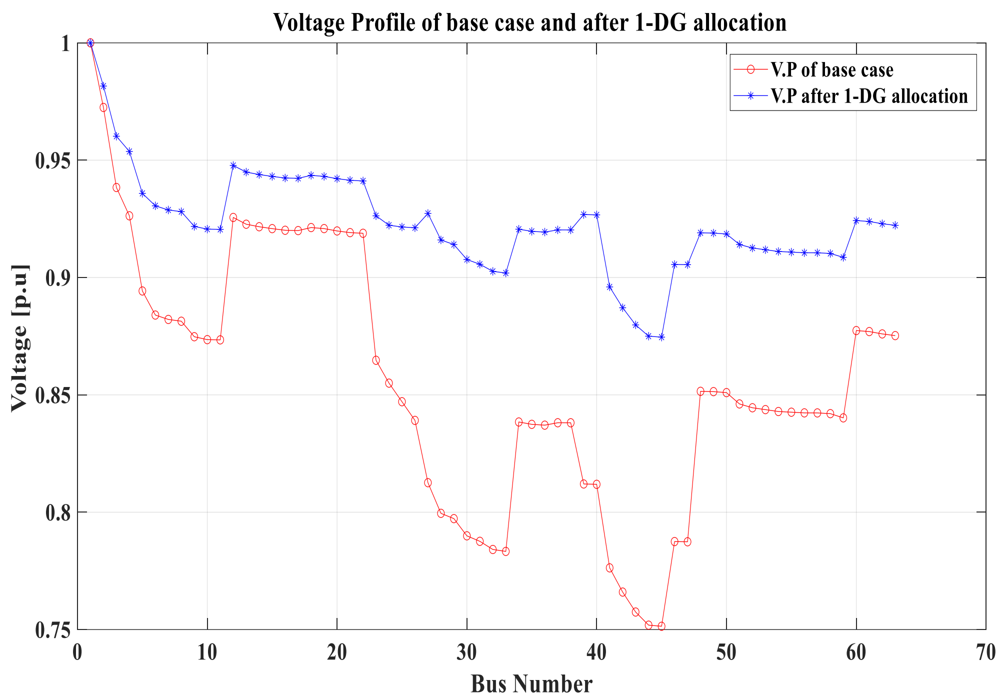

Figure 4.4: Voltage profile (p.u) after one DG is allocated

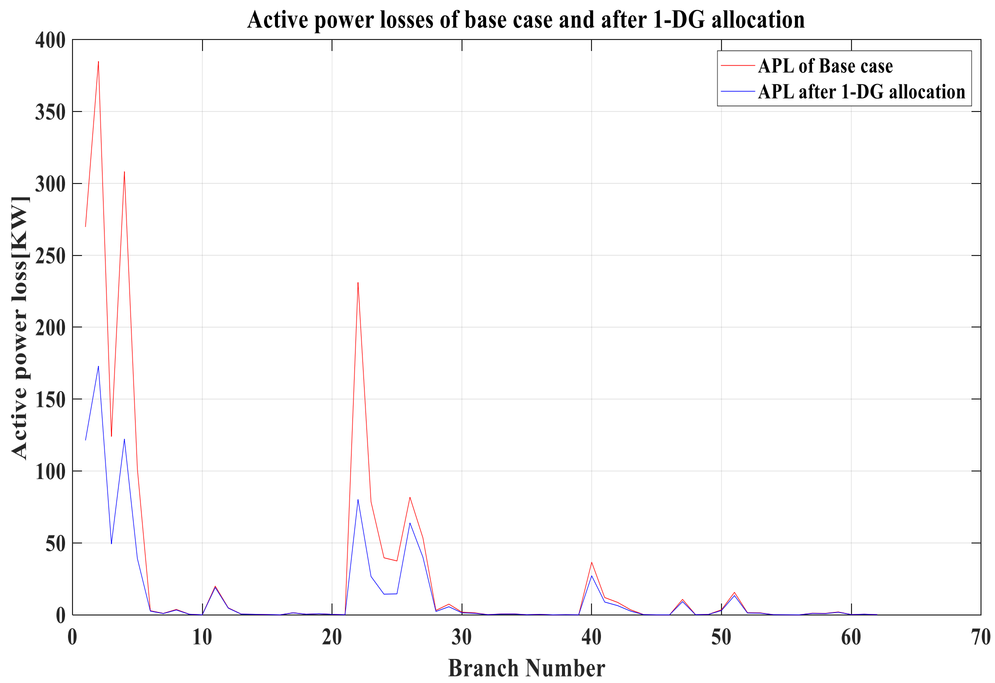

Figure 4.5: Active power loss (KW) after one DG is allocated

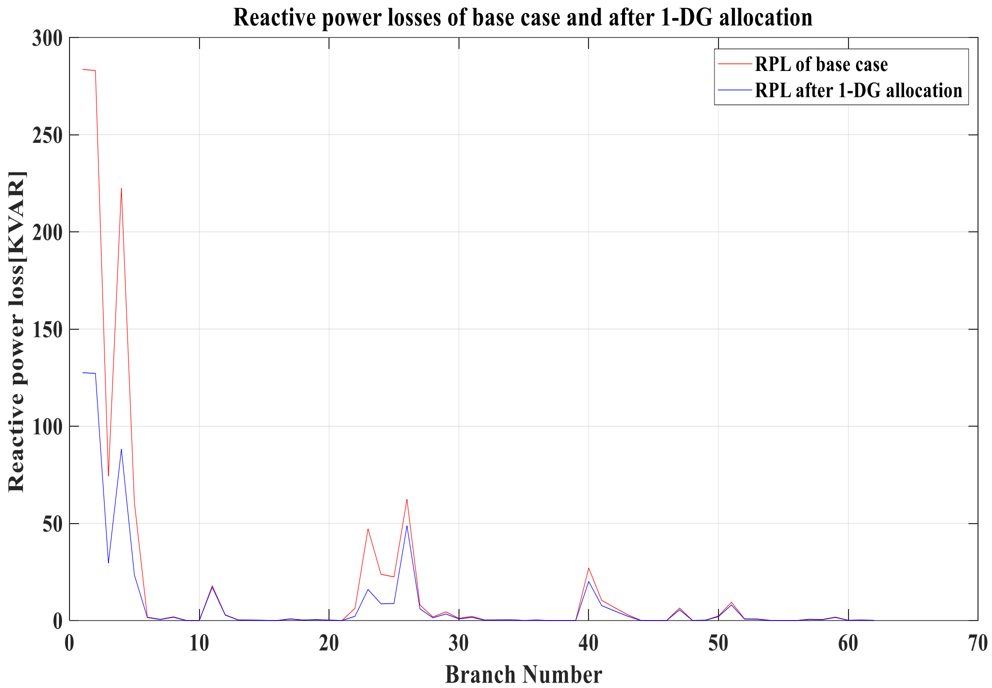

Figure 4.6: Reactive power loss (KVar) after one DG is allocated

Case III: System Performance with Four DG

A load flow simulation is conducted after integrating four DGs to assess the power system's network performance in this case. The best locations for DG placements are bus 13, 26, 41, and 54; their optimal sizes are 0.7122 MW, 1MW, 0.5592 MW, and 1 MW, respectively. The voltage profile of the network after four DGs are installed at buses 13, 26, 41, and 54 is presented in Figure 4.7 and the obtained active and reactive power losses are presented in Figures 4.8 and 4.9 respectively. In this instance, the lowest voltage is recorded at bus 45 with a value of 0.9227, which is lower than the threshold voltage limit (i.e. 0.95 p.u). In this instance, there are 24 buses whose voltages are lower than the rated limit. The total real and reactive power losses of the given system when four DGs are allocated are minimized to 597.6604 KW and 389.4869 kVar respectively.

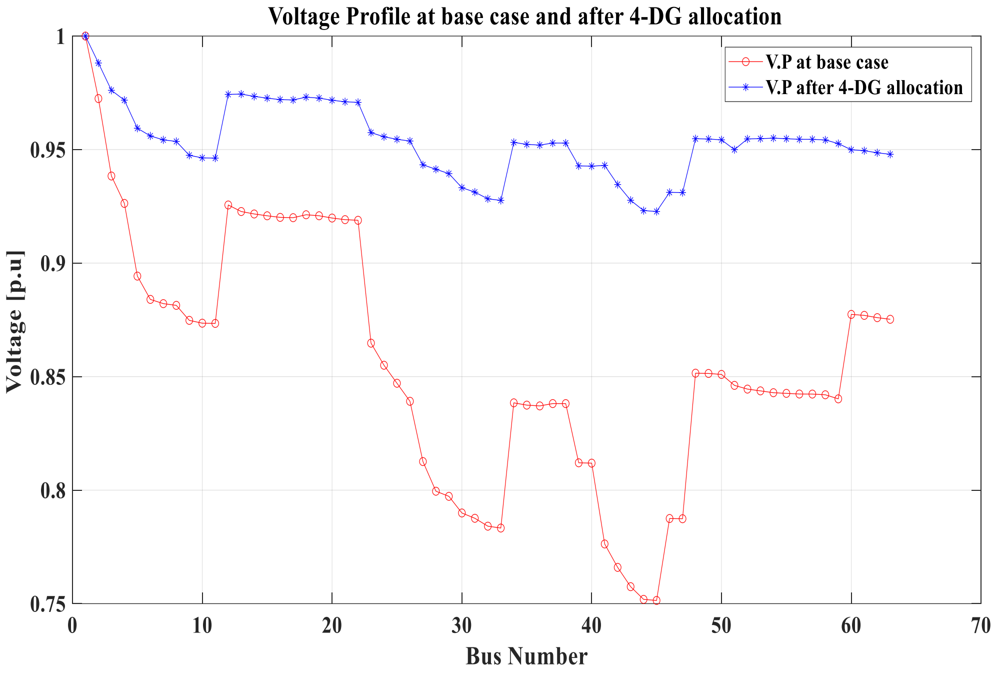

Figure 4.7: Voltage profile (p.u) after four DG are allocated

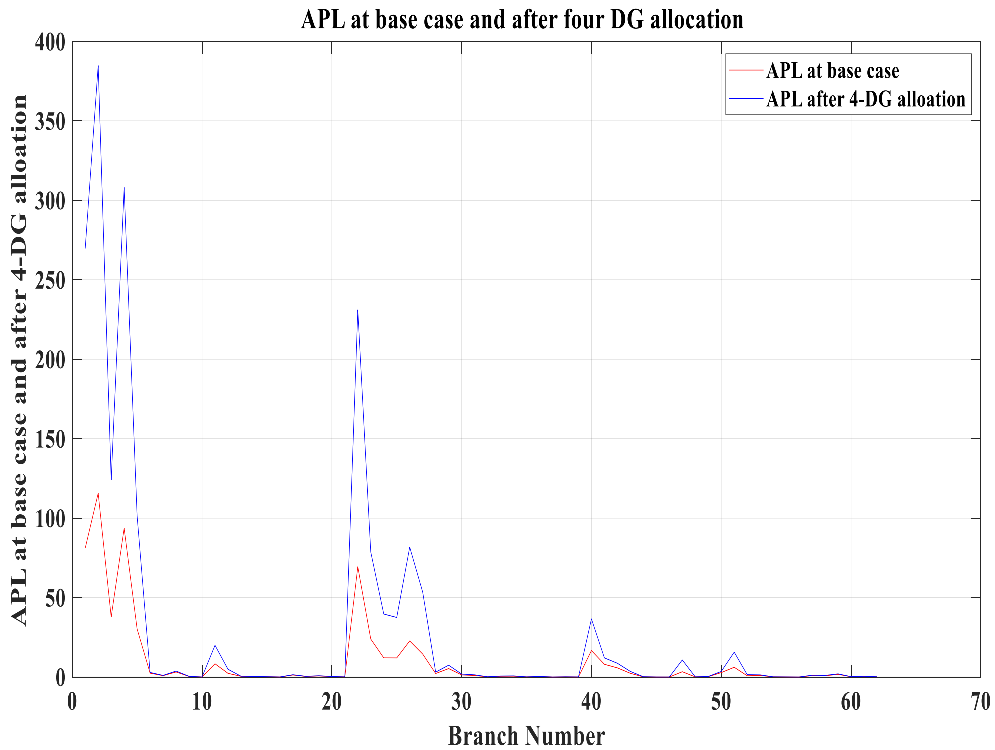

Figure 4.8: Active power loss (KW) after four DG is allocated

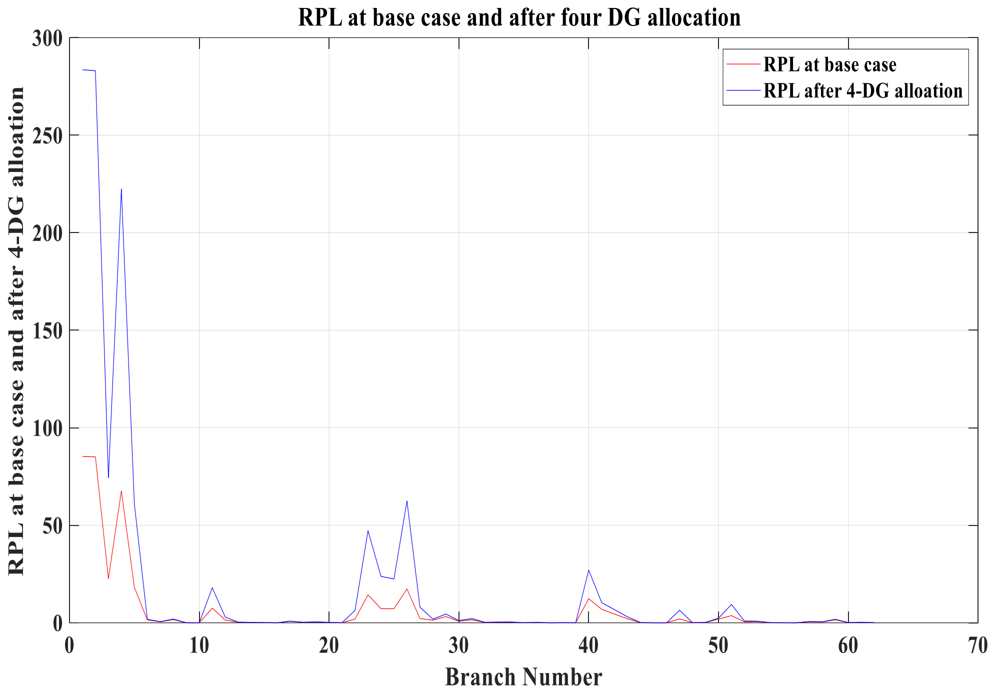

Figure 4.9: Reactive power loss (KVar) after four DG is allocated

Case IV: System Performance with three DG and one DSTATCOM

In this case, a load flow simulation is carried out after incorporating three DGs and one DSTATCOM to analyze the distribution system's performance. The optimal places for DGs are buses 41, 53, and 26, with optimal sizes of 0.6694 MW, 1 MW, and 1 MW, respectively. The best location for DSTATCOM placement is bus 28 and its optimal size is 1 MVAR. The voltage profile of the network after three DG and one DSTATCOM are installed at buses 41, 53, 26, and 28 respectively are presented in Figure 4.10 and, the obtained active and reactive power losses are presented in Figures 4.11 and 4.12 respectively. In this case, the minimum voltage is recorded at bus 45 having a value of 0.9544. In this case, the voltage level of each bus is within the allowable range. When three DGs and one DSTATCOM are allocated, the total active and reactive power losses are minimized to 285.656 KW and 203.709 kVar respectively.

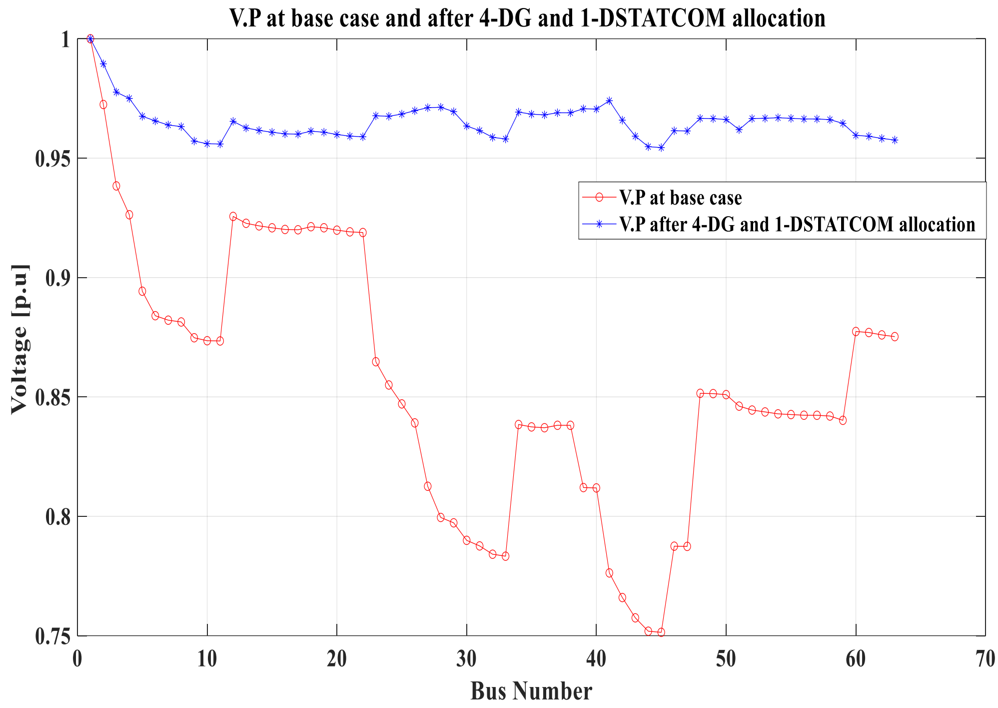

Figure 4.10: Voltage profile (p.u) after three DG and one DSTATCOM are allocated

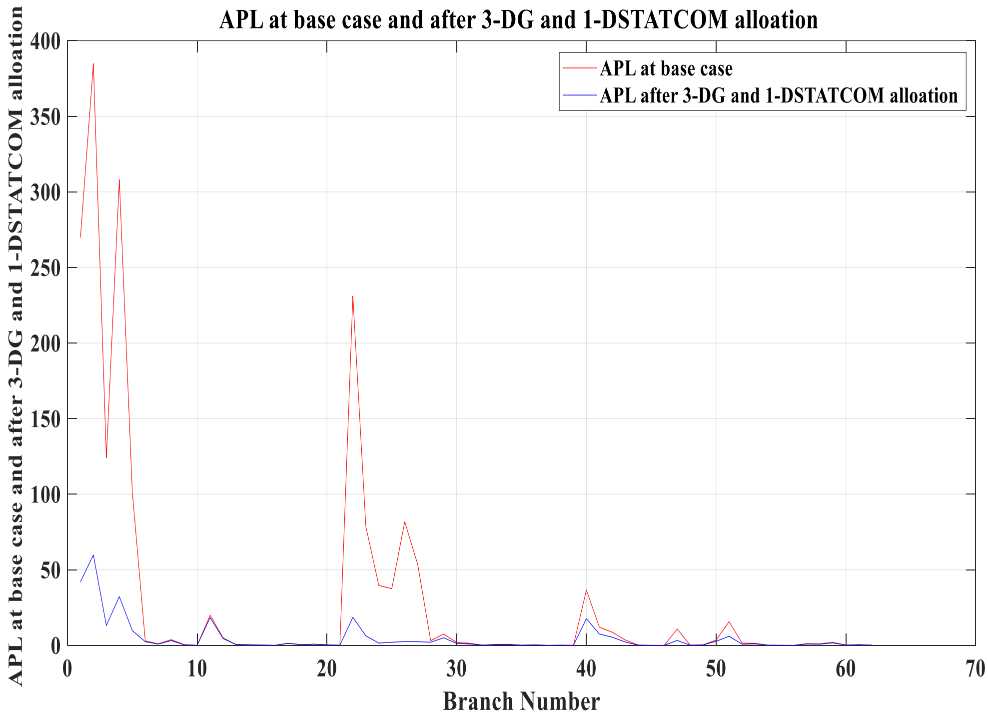

Figure 4.11: Active power loss (KW) after three DG and one DSTATCOM is allocated

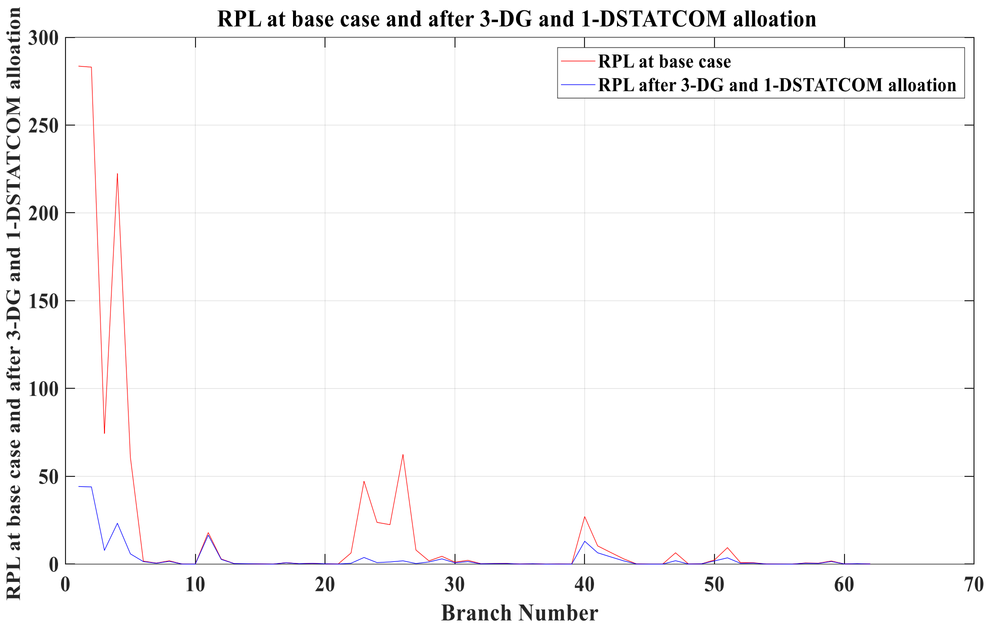

Figure 4.12: Reactive power loss (KVar) after three DG and one DSTATCOM is allocated

4.3. Result Comparison of Base Case, after 1-DG, 4-DG, 3-DG, and 1-DSTATCOM Integration

From the above analysis, at the base case, the lowest voltage profile is 0.75141 at bus 45, which is lower than the threshold voltage limit and the active and reactive power losses are 1862.9 KW and 1204.5 kVar respectively. When only the placement of a single DG is considered with the optimal place at bus 27 and optimal size 4 MW, the voltage profile is enhanced and the minimum voltage level is 0.8745 at bus 45. In addition, the active and reactive power loss is minimized to 870.0948 KW and 576.5648 kVar respectively. Even if the voltage profile is improved only four buses are within the acceptable range. When four DGs are placed at the optimal place of 13, 26, 41, and 54 buses and with optimal sizes of 0.7122 MW, 1MW, 0.5592 MW, and 1 MW, respectively, the voltage profile is enhanced and the lowest voltage level is 0.9227 at bus 45. In addition, the active and reactive power loss is minimized to 597.6604 KW and 389.4869 kVar respectively. Again, the total size of DG decreases to 3.2714 MW when compared with single DG integration. But, still now there are 24 buses whose voltages are below the rated limit. When three DGs and one DSTATOM are placed at the optimal place of 41, 53, and 26 buses and with optimal sizes of 0.6694 MW, 1MW, and 1 MW respectively, the voltage profile is enhanced and the minimum voltage level is 0.9544 at bus 45. In addition, the active and reactive power loss is decreased to 285.6559 KW and 203.7087kVAR respectively. In this case, the voltage level of each bus is within the permissible range.

Figure 4.13 presents the voltage profile of all buses in the radial distribution system under four distinct cases: (1) base case, (2) with one DG, (3) with four DGs, and (4) with three DGs and one DSTATCOM optimally placed in the system. Figure 4.13 clearly shows that only in the fourth case, where three DGs and one DSTATCOM are placed, do all buses maintain voltage levels within acceptable limits. This indicates that DG placement alone cannot adequately address reactive power needs and enhance the voltage profile. In the base case, the lowest voltage is 0.75141 p.u at bus 45. However, when three DGs and one DSTATCOM are integrated, this voltage value is improved significantly to 0.9544 p.u. Figures 4.14 and 4.15 illustrate the total real and reactive power losses under the four different cases. The combination of three DGs and one DSTATCOM results in the lowest losses in both active and reactive power among the other three cases.

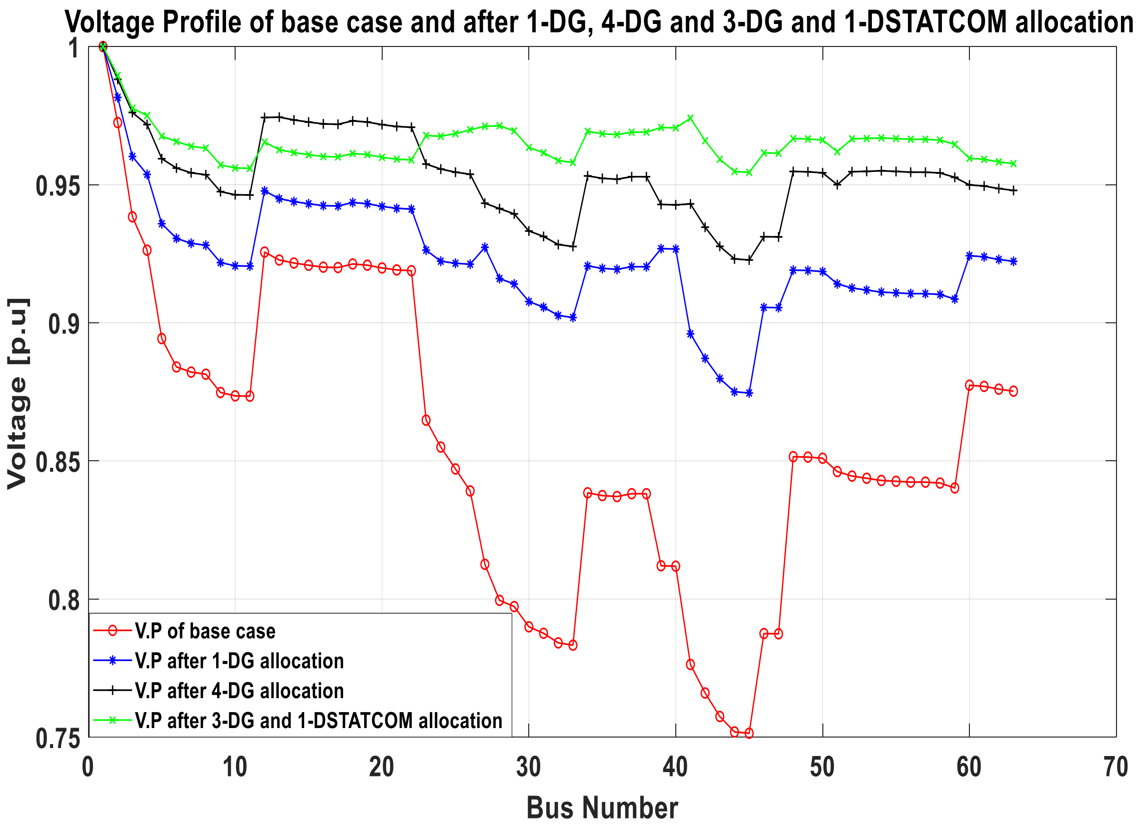

Figure 4.13: Voltage profile of the system in four distinct cases i.e. base case, with one DG only, with four DGs, and with three DG and one DSTATCOM

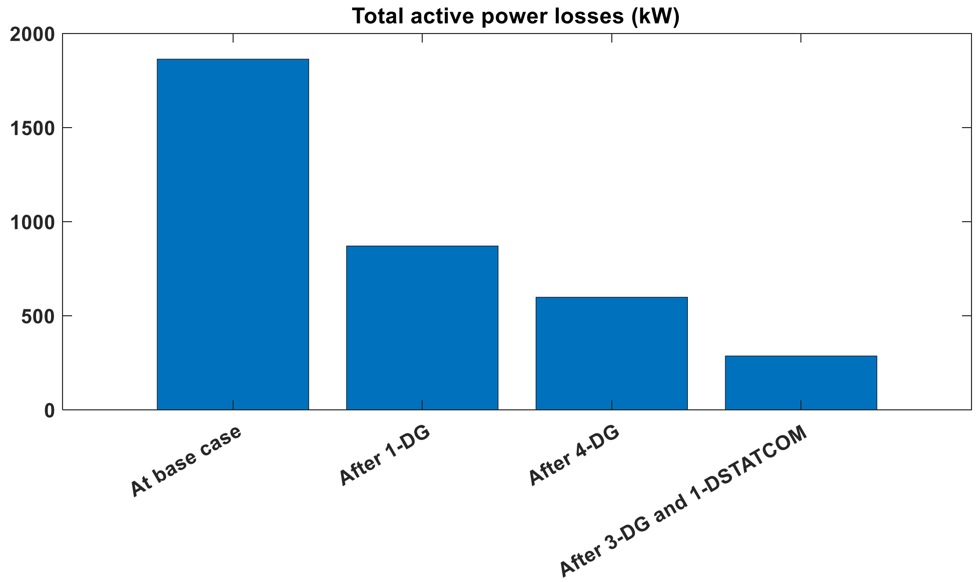

Figure 4.14: Total active power loss of the system in four distinct cases i.e. base case, with one DG, with four DGs, and with three DG and one DSTATCOM

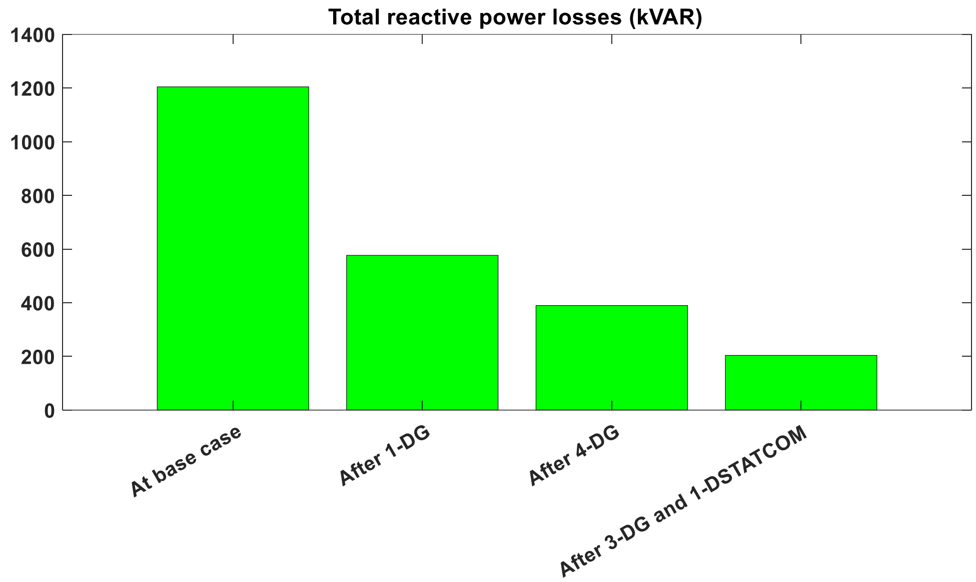

Figure 4.15: Total reactive power loss of the system in four distinct cases i.e. base case, with one DG, with four DGs, and with three DG and one DSTATCOM

Table 4.1: Summary of the simulation results under different cases

Description	Case I: Base case	Case II: With one DG	Case III: With four DG	Case IV: With three DG and one DSTATCOM
Size of DG (MW) (Position)	---	4 MW (27)	0.7122 MW @ 13, 1 MW @ 26, 0.5592 MW @ 41, 1 MW @ 54	0.6694 MW @ 41 1 MW @ 53 1MW @ 26
Size of DSTATCOM (MVAR) (Position)	---	---	---	1MVAR @ 28
Minimum V.P(p.u)	0.75141	0.8745	0.9227	0.9544
TAPL (KW)	1862.9	870.0948	597.6604	285.6559
TRPL (KVar)	1204.5	576.5648	389.4869	203.7087
Percentage of TAPL	---	53.29%	67.92%	84.67%
Percentage of TRPL	---	52.13%	67.66%	83.09%

4.4. Cost Analysis

4.4.1. DG and DTATCOM Investment Cost

DG Investment Cost

The investment cost of solar-based DG significantly changes from time to time. Based on the data obtained from (IRENA, 2019) the global investment cost of solar PV projects is expected to experience a significant decrease over the next three decades. The cost is projected to range between 490 to 985 USD/KW by 2018, 340 to 720 USD/kW by 2030, and further down to 165 to 481 USD/kW by 2050 (IRENA, 2019; Kefeni Getahun Shanko, 2023). In this study, taking into account year-to-year fluctuations in PV costs, it becomes possible to approximate the current PV investment cost using this reference. Consequently, the estimated average PV investment cost for 2024 is 852.5 USD/kW. Finally, considering the 4th case, the investment cost of DG is computed and presented in Table 4.2 below.

Table 4.2: DG investment cost

DG size (MW)	Price per KW ($)	Total price ($)
DG1 = 0.6694	852.5	570,664
DG2 = 1	852.5	852,500
DG3 = 1	852.5	852,500
Total		2,275,663.5

Using the exchange rate provided by the Commercial Bank of Ethiopia on April 19, 2024, which is 1 USD = 57.9568 ETB, the total investment cost for DG is calculated to be 2,275,663.5 USD, equivalent to 131,890,174.34 ETB.

DSTATOM Investment Cost

The investment cost for DSTATCOM is estimated to be 70 USD/kVar, which encompasses the installation cost (Lemma Girma, 2023). Finally, with the consideration of case-4, the cost of DSTATCOM is calculated as:

Investment cost of DSTATCOM (1 MVAR) = 1000 KVAR * 70 USD/KVAR

= 70,000 USD.

Based on the exchange rate provided by the Commercial Bank of Ethiopia on April 19, 2024, where 1 USD = 57.9568 ETB, the total investment cost for DSTATCOM in Ethiopian Birr is calculated as follows:

Total investment cost of DSTATCOM = 70,000 USD * 57.9568 ETB/USD = 4,056,975.99 ETB.

Thus, the total investment cost of 3-DG with the size of 0.6694, 1 and 1 MW, and 1-DSTATCOM with the size of 1MVAR is 135,947,150.34 ETB.

4.4.2. Cost of Energy Lost Due to Power Loss

The cost of energy loss is calculated using the energy rates set by the Ethiopian Electric Utility. The energy cost is 2 ETB/kWh, according to the tariff for Industrial Medium Voltage 15 kV. At a rate of 2 ETB/kWh, we can estimate the total cost incurred from energy loss resulting from power loss, as well as the cost savings realized from installing 3 DG units and 1 DSTATCOM device as follows:

I) The cost of energy lost at base case

The cost of energy lost due to power loss at base case i.e. before integrating DG and DSTATCOM into the system is calculated as follows:

Cost of energy lost due to power loss at base case = Power loss at base case (Kw)*Time (hr/yr) * Electric tariff (ETB/KWh).

$$= 1862.9\text{KW} * 8760\ \text{hr/yr} * 2\text{ETB/KWh} = 32{,}638{,}008\ \text{ETB/yr}.$$

II) The cost of energy lost after 3-DG and 1-DSTATCOM integration into the system

The cost of energy lost after 3-DG and 1-DSTATOM integration into the system is calculated as follows:

Cost of energy lost due to power loss after DG and DSTATCOM = Power loss after 3-DG and 1-DSTATOM (Kw)*Time (hr/yr) *Electric tariff (ETB/KWh).

$$= 285.6559\ \text{KW} * 8760\text{hr/yr} * 2\ \text{ETB/KWh} = 5{,}004{,}691.37\ \text{ETB/yr}.$$

III) Net profit due to 3-DG and 1-DSTATCOM integration into the system

The annual benefit after 3-DG and 1-DSTATCOM integration is the difference between the cost of energy lost due to power loss at the base case and, after 3-DG and 1-DSTATCOM integration and it is calculated as follows:

Net profit = Cost of energy lost due to power loss at the base case - Cost of energy lost due to power loss after DG and DSTATCOM.

$$= 32{,}638{,}008\ \text{ETB/yr} - 5{,}004{,}691.37\ \text{ETB/yr} = 27{,}633{,}316.63\ \text{ETB/yr}$$

IV) Payback period

The payback period is calculated by dividing the net investment of 3-DG and 1-DSTATOM cost by the annual net profit. Mathematically:

$$\text{Payback period} = \frac{\text{Net investment cost}}{\text{Annual net profit}}$$

$$= \frac{135{,}947{,}150.34\ \text{ETB}}{27{,}633{,}316.63\ \text{ETB/yr}} = 4.92\ yr \approx 4yr\ a\text{nd 11 months.}$$

Based on the financial assessment, the time it takes to recover the initial investment cost is approximately five years.

CHAPTER FIVE

5. CONCLUSIONS AND RECOMMENDATIONS

5.1. Conclusions

This thesis employs the Particle Swarm Optimization (PSO) method to find the optimal place and size of DG and DSTATCOM devices. The thesis aims to minimize real and reactive power losses and enhance the voltage profile in the Adama substation II feeder L2.

The base case MATLAB simulation results show that Adama substation II feeder L2 has substantial power losses and minimal voltage profile. Specifically, the feeder experiences a real power loss of 1862.9 kW, a reactive power loss of 1204.5 kVar, and a minimum voltage level of 0.75141. This thesis investigates the optimal placement of DGs and DSTATCOMs to enhance the system performance. When one DG is strategically placed at bus 27 with a capacity of 4 MW, the minimum voltage is increased to 0.8745. Additionally, the real and reactive power losses are effectively minimized by 53.29% and 52.3%, respectively. While the placement of DG can effectively reduce power losses in the system, it may not adequately address the reactive power demands of the network. This can result in under voltage at many buses. The optimal placement of DSTATCOM solves this under-voltage problem. When three DGs and one DSTATCOM are strategically placed at buses 13, 26, 41, and 54, respectively, with optimized sizes of 0.7122 MW, 1 MW, 0.5592 MW, and 1 MW, the voltage profile is significantly enhanced, with a lowest voltage of 0.9544 at bus 45. Additionally, the real and reactive power losses are effectively reduced by 84.67% and 83.09%, respectively. Notably, all buses maintain voltage levels within acceptable limits. Based on this research results, instead of using multiple DG units, its more effective to utilize the combination of DG and DSTATCOM to achieve optimal results. This approach leverages the strengths of both technologies, where DG provides distributed energy generation, while DSTATCOM enhances voltage stability and power stability, leading to improved overall performance of the distribution system. By startegically integrating both DG and DSTATCOM, we can achieve a more efficient and reliable power system with reduced power loss and better voltage profiles.

Finally, an economic analysis was performed to evaluate the financial viability of the proposed solution. The economic analysis indicates that an investment of 135,947,179.31 ETB is required to install three DGs and one DSTATCOM at the optimal locations (buses 13, 26, 41, and 54) with optimal sizes of 0.7122 MW, 1 MW, 0.5592 MW, and 1 MW, respectively. The payback period analysis indicates that approximately 4.9 years are required to recover the investment. This implies that installing DG and DSTATCOM devices is economically viable and will enhance the performance of the Adama substation II feeder L2.

5.2. Recommendations

This research work is beneficial to different parties both directly and indirectly.

Based on the results of this thesis work, it is recommended that Ethiopian Electric Utility (EEU) use DG to minimize the power loss and DSTATCOM to enhance the voltage profile on Adama substation II feeder L2. This thesis contributes to Ethiopian Electric Utility's efforts to reduce both real and reactive power losses within their networks. Furthermore, this thesis contributes to the improvement of voltage levels at consumer premises, ensuring they meet the required limits. By doing so, the EEU and Ethiopian Electric Power (EEP) can avoid the costs associated with compensating customers for damaged equipment resulting from voltage deviations beyond acceptable ranges. This, in turn, enhances the economic viability and reliability of these companies' operations.

5.3. Future Works

Suggested future research directions to enhance this work include the following:

- Including the cost function and other power system factors, such as voltage stability, the objective function may be made better.
- Electric cars have gained popularity in recent times, and thus, future studies should consider incorporating electric vehicle (EV) charging stations along with the optimal allocation of DG and DSTATCOM.
- In this study, only PV-type DG was taken into consideration. It is recommended as future work to investigate alternative distributed generation for improving feeder voltage profile and reducing power loss. Also, further detail of cost analysis is recommended for future work.

REFERENCES

Abayneh, B., & Fekadu Shewarega, I. (2022). *Study on the Power Loss Reduction and Voltage Profile Improvement of Kotebe Distribution System by Optimal Placement of D-STATCOM Using a Hybrid of Genetic Algorithm and Particle Swarm Optimization Method*.

Adefarati, T., & Bansal, R. C. (2016). Integration of renewable distributed generators into the distribution system: A review. *IET Renewable Power Generation*, *10*(7), 873–884. https://doi.org/10.1049/IET-RPG.2015.0378

Aditya Prasad Padhy. (2020). Optimal Allocation and Size Selection of Dispersed Generation in Radial Distribution System. *International Journal of Engineering Research And*, *V9*(07). https://doi.org/10.17577/IJERTV9IS070036

Alwazni, H., & Al-kubragyi, S. (2021). Enhancement of an Iraqi Radial Distribution System Performance Using Multi-Object Particle Swarm Optimization. *Engineering and Technology Journal*, *39*(10), 1528–1538. https://doi.org/10.30684/etj.v39i10.2095

Alyu, A. B., Beshr, A., & Student, A. M. (2023). *A Review on Performance Enhancement of Distribution System Using Optimal Placement and Size of Distributed Generation and D-STATCOM*. https://www.researchgate.net/publication/371695133

Amin, A., Kamel, S., & Yu, J. (2019). Developed Analytical Technique for Optimal Placement and Sizing of DG and DSTATCOM in Radial Distribution Systems. *2018 20th International Middle East Power Systems Conference, MEPCON 2018 - Proceedings*, 1087–1091. https://doi.org/10.1109/MEPCON.2018.8635168

Bilgundi, S. K. (2020). Optimal placement and sizing of DG and DSTATCOM in a Radial Distributed Systems Based on Analytical Technique. In *SSRG International Journal of Electrical and Electronics Engineering (SSRG-IJEEE)* (Vol. 7). www.internationaljournalssrg.org

Devabalaji, K. R., & Ravi, K. (2016). Optimal size and siting of multiple DG and DSTATCOM in radial distribution system using Bacterial Foraging Optimization Algorithm. *Ain Shams Engineering Journal*, *7*(3), 959–971. https://doi.org/10.1016/J.ASEJ.2015.07.002

Ferminus Raj, A., & Gnana Saravanan, A. (2023). An optimization approach for optimal location & size of DSTATCOM and DG. *Applied Energy*, *336*. https://doi.org/10.1016/j.apenergy.2023.120797

Gad, A. G. (2022). Particle Swarm Optimization Algorithm and Its Applications: A Systematic Review. *Archives of Computational Methods in Engineering*, *29*(5), 2531–2561. https://doi.org/10.1007/s11831-021-09694-4

Gana, N. N., & Akpootu, D. O. (2013). Estimation of global solar radiation using four sunshine based models in Kebbi, North-Western, Nigeria. *Pelagia Research Library Advances in Applied Science Research*, *4*, 409–421. www.pelagiaresearchlibrary.com

Getie, B., & Dar, B. (2019). *Improvement of Distribution System Reliability Using Distributed Generation and Circuit Recloser (Case Study: Motta Substation)*.

Hingorani, N. G., Gyugyi, Laszlo., & El-Hawary, M. E. (2000). *Understanding FACTS : concepts and technology of flexible AC transmission systems*. IEEE Press.

Iqbal, F., Khan, M. T., & Siddiqui, A. S. (2018). Optimal placement of DG and DSTATCOM for loss reduction and voltage profile improvement. *Alexandria Engineering Journal*, *57*(2), 755–765. https://doi.org/10.1016/j.aej.2017.03.002

IRENA. (2019). *Future of solar photovoltaic : deployment, investment, technology, grid integration and socio-economic aspects (A Global Energy Transformation: paper), International Renewable Energy Agency, Abu Dhabi*.

Isha, G., Jagatheeswari, P., & Jasmine Gnana Malar, A. (2023). Elitist Harris Hawks Optimized Voltage Stability Enhancement in Radial Distribution System. *Journal of Electrical Engineering and Technology*, *18*(4), 2683–2693. https://doi.org/10.1007/s42835-023-01375-5

Kaushal, J., & Basak, P. (2019). Frequency control of islanded microgrid using fuzzy-PI and autotuned controllers. *International Journal of Advances in Applied Sciences*, *8*(1), 64–72. https://doi.org/10.11591/ijaas.v8.i1.pp64-72

Kefeni Getahun Shanko. (2023). *Reliability Improvement and Power Loss Reduction in Distribution Substation Via Distributed Generation (Case study: Hormat Substation II)*.

Kidane Tsehay Asrat. (2023). *Investigation and Voltage Profile Improvement by using D-STATCOM as FACTS Devices in Power Distribution System (A Case Study Welenchiti city Distribution system)*.

Kongming Sun, Yudun Li, Xin Wang, Naiyong Li, Rongqi Fan, Guohui Zhang, & Meng Liu. (2020). *Photovoltaic Power Station Modeling and Its Impact on Distribution Networks*.

Kumar Pujari, H. (2020). Optimization Techniques and Algorithms for DG placement in Distribution System: A Review. *Mageshvaran R International Journal on Emerging Technologies*, *11*(3), 141–157. www.researchtrend.net

Lasmari, A., Zellagui, M., Chenni, R., Semaoui, S., El-Bayeh, C. Z., & Hassan, H. A. (2020). Optimal energy management system for distribution systems using simultaneous integration of PV-based DG and DSTATCOM units. *Energetika*, *66*(1), 1–14. https://doi.org/10.6001/ENERGETIKA.V66I1.4294

Lemma Girma. (2023). *Comparative Studies of FACTS Devices for Power Loss Reduction and Voltage Profile Improvement in Radial Distribution Systems (Case Study: Sebbata-I Substation Outgoing Feeder)*.

Mandefro, E. (2019). *Performance Enhancement Of Distribution System Using Optimally Allocated Distributed Generation: - A Case Study On Bahir Dar Power Distribution*. http://hdl.handle.net/123456789/10379

Maurya, A., & Sharma, A. K. (2023). Optimal Placement and Sizing of DG and D-STATCOM in Radial Distribution System Using Arithmetic Optimization Algorithm. *2023 IEEE 8th International Conference for Convergence in Technology, I2CT 2023*. https://doi.org/10.1109/I2CT57861.2023.10126404

Mehammed, A. (2017). *Reliability Assessment Of Distribution System And Improvement By Intelligent Placement Of Distributed Generation (Dg) On Case Study Of Gonder City Power Distribution System.* http://hdl.handle.net/123456789/10785

Mesgana Tulu. (2023). *Design and Optimization of Grid-connected Solar Powered Electric Vehicle Charging Station (Case Study of Adama City)*.

Mihret Desta. (2019). *Voltage and Reactive Power Control for Power Loss Minimization of Distribution Networks Voltage and Reactive Power Control for Power loss*

Minimization of Distribution Networks Case Study-(Sebeta I Substation Outgoing Feeder).

Pandey, D., & Singh Bhadoriya, J. (2014). Optimal Placement & Sizing Of Distributed Generation (DG) To Minimize Active Power Loss Using Particle Swarm Optimization (PSO). *INTERNATIONAL JOURNAL OF SCIENTIFIC & TECHNOLOGY RESEARCH*, *3*(7). www.ijstr.org

Reddy, G. H., Koundinya, A. N., Gope, S., Raju, M., & Singh, K. M. (2022). Optimal Sizing and Allocation of DG and FACTS Device in the Distribution System using Fractional Lévy Flight Bat Algorithm. *IFAC-PapersOnLine*, *55*(1), 168–173. https://doi.org/10.1016/J.IFACOL.2022.04.028

Salkuti, S. R. (2021). Optimal Allocation of DG and D-STATCOM in a Distribution System using Evolutionary based Bat Algorithm. *International Journal of Advanced Computer Science and Applications*, *12*(4), 360–365. https://doi.org/10.14569/IJACSA.2021.0120445

Sarabia, A. F. (2011). *Impact of distributed generation on distribution system Title: Impact of Distributed Generation on Distribution System Semester: 10 th*.

Taha, W. (2014). Comparative study between wind and photovoltaic (PV) systems. *Springer Proceedings in Physics*, *155*, 419–430. https://doi.org/10.1007/978-3-319-05521-3_54

Taye, T. (2019). *Improvement of Distribution Feeder Loss and Voltage Profile (Case Study: Bella Substation Distribution Feeder)*.

Teng, J. H. (2003). A direct approach for distribution system load flow solutions. *IEEE Transactions on Power Delivery*, *18*(3), 882–887. https://doi.org/10.1109/TPWRD.2003.813818

Tungadio, D. H., Numbi, B. P., Siti, M. W., & Jimoh, A. A. (2015). Particle swarm optimization for power system state estimation. *Neurocomputing*, *148*, 175–180. https://doi.org/10.1016/j.neucom.2012.10.049

Witoon Prommee, & Weerakorn Ongsakul. (2008). *Optimal Multi-Distributed Generation Placement by Adaptive Weight Particle Swarm Optimization*.

Yuvaraj, T., & Ravi, K. (2018). Multi-objective simultaneous DG and DSTATCOM allocation in radial distribution networks using cuckoo searching algorithm. *Alexandria Engineering Journal*, *57*(4), 2729–2742. https://doi.org/10.1016/J.AEJ.2018.01.001

APPENDICES

MATLAB Code for BIBC and BCBV Creation

```
%% Creating BIBC and BCBV Matrix
function [BIBC_matrix, BCBV_matrix] = Create_BIBC_BCBV(LD, BD)
   [LD, BD]=linedata; %Call the LineData fun to import line data and bus data

   %% BASE VALUE INITIALIZATION AND CALCULATION
   MVAb=100;              %base MVA
   KVb=15;                %base kV
   Zb=(KVb^2)/MVAb;   %base impedance

   %% determining the total number of buses and branches
   br=length(LD(:,1));      % number of branch
   no=length(BD(:,1));      % number of buses

   % Convert Resistance and Reactance value to per-unit values
   for i=1:br
      R(i,1)=(LD(i,4))/Zb;
      X(i,1)=(LD(i,5))/Zb;
   end

   % Initialize BIBC matrix
   BIBC_matrix = zeros(br, no - 1);
   i = 1;
   j = 1;
   % filling the BIBC matrix
   while i <= br
      x = LD(i, 2);     % Sending end node
      y = LD(i, 3);     % Receiving end node
      while x~=LD(j,2)
         j=j+1;
      end
      if x == 1
         BIBC_matrix(y - 1, i) = BIBC_matrix(y - 1, i) + 1;
         i = i + 1;
      else
         BIBC_matrix(:, i) = BIBC_matrix(:, j - 1);
         BIBC_matrix(y - 1, i) = BIBC_matrix( y - 1, i) + 1;
         i = i + 1;
      end
      j=1;
   end
```

```
    % Initialize BCBV matrix
    BCBV_matrix = zeros(no - 1, br);
    i = 1;
    j=1;
    % filling the BCBV matrix
    while i <= br
        x = LD(i, 2);          % Sending end node
        y = LD(i, 3);          % Receiving end node
        while x~=LD(j,2)
            j=j+1;
        end
        if x == 1
            BCBV_matrix(i, y - 1) = R(i, 1) + 1i * X(i, 1);
            i = i + 1;
        else
            BCBV_matrix(i,:) = BCBV_matrix(j - 1, :);
            BCBV_matrix(i, y - 1) = R(i, 1) + 1i * X(i, 1);
            i = i + 1;
        end
        j=1;
    end
end
```

MATLAB Code for Base Case Load Flow

```
function [SLT, VP,SLT_base_each]=loadflow_base_case
%function calling
[LD,BD]=linedata;
[BIBC_matrix, BCBV_matrix] = Create_BIBC_BCBV(LD, BD);

%initializing base value
MVAb=100;             %base MVA
KVb=15;               %base kV
Zb=(KVb^2)/MVAb;      % base impedance

%ideftifying the sending bus(left node) and recieving bus(right node)
nl=LD(:,2);           % left node
nr=LD(:,3);           % right node

%determining the branch number and bus number
br=length(LD(:,1));    % number of branch
no=length(BD(:,1));    % number of buses

% converting resistance and reactance to per-unit Values
```

```
for i=1:br
   R(i,1)=(LD(i,4))/Zb;
   X(i,1)=(LD(i,5))/Zb;
end

% converting active(P) and reactive power(Q) to per-unit values
for i=1:no
   P(i,1)=((BD(i,2))/(1000*MVAb));
   Q(i,1)=((BD(i,3))/(1000*MVAb));
end

%calculating impedance value from R and X
Z = complex(R(:,1),X(:,1));

%calculating the DLF matrix
DLF_matrix = BCBV_matrix * BIBC_matrix;

%initializing I(node current), V(Voltage), and reference voltage
I = zeros((no-1), 1);
V = zeros((no-1), 1);
V_r = ones(no-1,1);
Vs=1+1i*0;          %Voltage of slack bus

%initializing the iteration and tolerance
iter = 100;
tolerance = 1;

%Calculate the node current injection matrix
while tolerance > 10^-12
   for i = 2:no
      sload=complex(P(i,1),Q(i,1));
      I(i-1,1) = conj(sload/V_r(i-1,1));
   end
   deltaV = DLF_matrix*I;
   for j = 1:(no-1)
     V(j,1) = Vs - deltaV(j, 1);
   end
   for i=1:br
     tol(i,1)=V(i,1) - V_r(i,1);
   end
   tolerance = max(abs(tol));
   V_r = V;
 end
```

```
%this is one to add the V1(slack bus voltage) to VP
for i=1:no
 if i==1
     VP(1,1)=1+1i*0;
 else
     VP(i,1)=V(i-1, 1);
 end
end

SLT = 0;        %initialize the total power loss of the base case
%calculating the power loss between two buses
for n = 1:br
    m = nl(n,1);
    k = nr(n,1);
    In = (VP(m) - VP(M))/Z(n);
    Ik = (VP(k) - VP(m))/Z(n);
    Snk = VP(m)*conj(In)*100000;
    Skn = VP(k)*conj(Ik)*100000;
    SL  = Snk + Skn;
    SLT = SLT + SL;
    SLT_base_each(n)=SL;
end

figure(2);
plot(abs(VP),'red');
hold off;
title('Voltage Profile at Base Case');
grid on;
xlabel('Bus Number') ;
ylabel('Voltage [p.u]') ;
legend('Base case voltage profile');

figure(3);
plot(real(SLT_base_each),'red');
hold off;
title('Active power loss at base case');
grid on;
xlabel('Branch Number');
ylabel('Active power loss');
legend('Active power loss (KW)');

figure(4);
plot(imag(SLT_base_each),'blue');
hold off;
```

```
title('Reactive power loss at base case');
grid on;
xlabel('Branch Number');
ylabel('Reactive power loss');
legend('Reactive power loss (KVAR)');
end
```

MATLAB Code for Load Flow with DG and DSTATCOM

```
function [VP_dg_ds, SLT_dg_ds,SLT_each]=loadflowwith_dg_dstatcom(x, ndg)
%function calling to read the line data and bus data
[LD, BD]=linedata;
[BIBC_matrix, BCBV_matrix] = Create_BIBC_BCBV(LD, BD);

%initializing base value
MVAb=100;            %base MVA
KVb=15;              %base kV
Zb=(KVb^2)/MVAb;       % base impedance

%ideftifying the sending bus(left node) and recieving bus(right node)
nl=LD(:,2);           % left node
nr=LD(:,3);           % right node

%determining the branch number and bus number
br=length(LD(:,1));     % number of branch
no=length(BD(:,1));     % number of buses

% converting resistance and reactance to per-unit values
for i=1:br
   R(i,1)=(LD(i,4))/Zb;
   X(i,1)=(LD(i,5))/Zb;
end

% converting active(P) and reactive power(Q) to per-unit values
for i=1:no
   P(i,1)=((BD(i,2))/(1000*MVAb));
   Q(i,1)=((BD(i,3))/(1000*MVAb));
end

%Placing DG and DSTATCOM at the appropriate place
for i=1:ndg-1
   P(round(x(i)),1)=P(round(x(i)),1)-(x(ndg+i))/(1000*MVAb);
end
for i=ndg:ndg
```

```
    Q(round(x(i)),1)=Q(round(x(i)),1)-(x(ndg+i))/(1000*MVAb);
end

%calculating impedance value from R and X
Z = complex(R(:,1),X(:,1));

%calculating the DLF matrix
DLF_matrix = BCBV_matrix * BIBC_matrix;

%initializing I(node current), V(Voltage), and reference voltage
I = zeros((no-1), 1);
V = zeros((no-1), 1);
V_r = ones(no-1,1);
Vs=1+1i*0;          %Voltage of slack bus

%initializing the iteration and tolerance
iter = 100;
tolerance = 1;

%Calculate the node current injection matrix
while tolerance > 10^-12
    for i = 2:no
       sload=complex(P(i,1),Q(i,1));
       I(i-1,1) = conj(sload/V_r(i-1,1));
    end
    deltaV = DLF_matrix*I;
    for j = 1:(no-1)
      V(j,1) = Vs - deltaV(j, 1);
    end
    for i=1:br
      tol(i,1)=V(i,1) - V_r(i,1);
    end
    tolerance = max(abs(tol));
    V_r = V;
 end

%this is one to add the V1(slack bus voltage) to VP
for i=1:no
  if i==1
      VP_dg_ds(1,1)=1+1i*0;
  else
      VP_dg_ds(i,1)=V(i-1, 1);
  end
end
```

```
SLT_dg_ds = 0;       %initialize the total power loss after dg and dstatcom
%calculating the power loss between two buses
for n = 1:br
   m = nl(n,1);
   k = nr(n,1);
   In = (VP_dg_ds(m) - VP_dg_ds(k))/Z(n);
   Ik = (VP_dg_ds(k) - VP_dg_ds(m))/Z(n);
   Snk = VP_dg_ds(m)*conj(In)*100000;
   Skn = VP_dg_ds(k)*conj(Ik)*100000;
   SL  = Snk + Skn;
   SLT_each(n)=SL;
   SLT_dg_ds = SLT_dg_ds + SL;
end
end
```

MATLAB Code for Fitness Function

```
function f = confun(x)
   ndg=numel(x)/2;
   [VP_dg_ds, SLT_dg_ds,SLT_each]=loadflowwith_dg_dstatcom(x,ndg);
   f1(1)=0;
   f1(2)=0;
   f1(3)=0;
   f1(1)=real(SLT_dg_ds);
   f1(2)=imag(SLT_dg_ds);
   f1(3)=(sum(1-abs(VP_dg_ds)).^2);

   % Define weights for for objective funtions. These weights must sum to unity
   w1=0.5;       %Weights value for active power loss
   w2=0.1;       %Weights value for reactive power loss
   w3=0.4;       %Weights value for voltage deviation

   % minimization of objective function
   f= 0.5*f1(1) + 0.1*f1(2) + 0.4*f1(3);
end
```

Main PSO Program for Optimization of Constrained Problem

```
% main PSO program for optimization of constrained problem
tic
clear all
close all

%Setup PSO parameters
```

```
ndg=4;
nvars=ndg*2;           %Num of Variables(2*num DG).. Optimize both location and size
lb=zeros(1,nvars);      %Define lower bound
lb(1:ndg)=2;           %Lower bound of location is 2, 1 is feederbus
lb(ndg+1:2*ndg)=100;    %Lower bound of Size defined by user
ub=zeros(1,nvars);      %Define upper bound
ub(1:ndg)=63;           %Upper bound of location is the last bus (33 or 69)
ub(ndg+1:2*ndg)=2500;   %Upper bound of Size defined by user
% PSO Settings
% Visit <https://www.mathworks.com/help/gads/particleswarm.html> for more info
options = optimoptions('particleswarm','PlotFcn',@pswplotbestf);
obj_func=@(x)confun(x);    %Chama FO
rng default  % For reproducibility
[x,fval,exitflag,output] = particleswarm(obj_func,nvars,lb,ub,options);
x(1:ndg)=round(x(1:ndg));   % Apply integer condition for location

% %run the load flow of base case
[SLT, VP,SLT_base_each]=loadflow_base_case;

%run the load flow analayssis after DG and DSTATCOM placement
[VP_dg_ds, SLT_dg_ds,SLT_each]=loadflowwith_dg_dstatcom(x,ndg);
disp('Active Power Loss After DG and DSTATCOM')
disp(real(SLT_dg_ds));
disp('Reactive Power Loss after DG and DSTATCOM')
disp(imag(SLT_dg_ds))

disp('Bus No     DG Size(kW)');
disp([x(1:ndg-1)', x(ndg+1:nvars-1)']);
disp('Bus No     DSTATOM Size(kVAR)');
disp([x(ndg:ndg)', x(nvars:nvars)']);

figure(2);
plot(abs(VP),'red');
hold on;
plot(abs(VP_dg_ds),'blue');
hold off;
title('V.P at base case and after 4-DG and 1-DSTATCOM allocation');
grid on;
xlabel('Bus Number') ;
ylabel('Voltage [p.u]') ;
legend('V.P at base case','V.P after 4-DG and 1-DSTATCOM allocation');

figure(3);
losses=[sum(real(SLT)); sum(real(SLT_dg_ds))];
```

```
legends=categorical({'Initial losses', 'After allocation of DG and DSTATCOM'});
legends = reordercats(legends,{'Initial losses', 'After allocation of DG and DSTATCOM'});
bar(legends,losses);
title('Total active power losses (kW)');

figure(4);
losses=[sum(imag(SLT)),sum(imag(SLT_dg_ds))];
legends=categorical({'Initial losses', 'After allocation of DG and DSTATCOM'});
legends = reordercats(legends,{'Initial losses', 'After allocation of DG and DSTATCOM'});
bar(legends,losses,'g');
title('Total reactive power losses (kVAR)');

figure(5);
plot(real(SLT_base_each),'red');
hold on;
plot(real(SLT_each),'blue');
hold off;
title('RPL at base case and after 3-DG and 1-DSTATCOM allocation);
grid on;
xlabel('Branch Number') ;
ylabel('APL at base case and after 3-DG and 1-DSTATCOM allocation) ;
legend('APL at base case', 'APL after 3-DG and 1-DSTATCOM allocation');

figure(6);
plot(imag(SLT_base_each),'red');
hold on;
plot(imag(SLT_each),'blue');
hold off;
title('RPL at base case and after 3-DG and 1-DSTATCOM allocation);
grid on;
xlabel('Branch Number') ;
ylabel('RPL at base case and after 3-DG and 1-DSTATCOM allocation) ;
legend('RPL at base case', 'RPL after 3-DG and 1-DSTATCOM allocation');
```